Ding, J., & Sperling, G. (2007). Binocular combination: Measurements and a model. In L. R. Harris & M. R. M. Jenkin (Eds.), *Computational vision in neural and machine systems* (pp. 257 - 305). Cambridge, UK: Cambridge University Press.

# 15 Binocular combination: measurements and a model

Jian Ding and George Sperling

## 15.1 Introduction

### 15.1.1 Cyclopean image

When different stimuli are presented to the left and right eyes, only a single, combined image is perceived, often called the *cyclopean image* after Cyclops, the one-eyed mythological monster. When the images in the left and right eyes are similar (compatible), the cyclopean image is a combination of the two. This chapter is concerned with the early visual processes that determine the proportion that each eye's image contributes to the cyclopean image. When the images in the left and right eyes are dissimilar (incompatible), such as a vertical grating in one eye and a horizontal grating in the other, or a positive image in one eye and its negative in the other, then typically within any small area of the visual field, only one of the two images is perceived. This phenomenon is called *binocular rivalry*. Although the processes of binocular combination and binocular rivalry share early stages of visual processing, we are here concerned only with the laws governing binocular combination.

#### Vector summation of same-wavelength monocular sinewave gratings

To obtain experimental data that yield the quantitative parameters of binocular combination, we take advantage of a simple mathematical fact. The arithmetic sum of two sine waves of the same wavelength is again a sine wave whose amplitude and phase are dependent on the phases and amplitudes of the two component sine waves. As shown in Figure 15.1, a sine wave can be represented as a vector, and the arithmetic summation of two sine waves of the same wavelength can be represented by vector summation. If $\vec{L}_\phi$ and $\vec{R}_\phi$ represent two sinewave gratings (in this example, images in the left and right eyes, respectively), the vector sum, $\vec{B}_\phi$, represents the sum of the two

*Computational Vision in Neural and Machine Systems*, ed. L. Harris and M. Jenkin. Published by Cambridge University Press. 

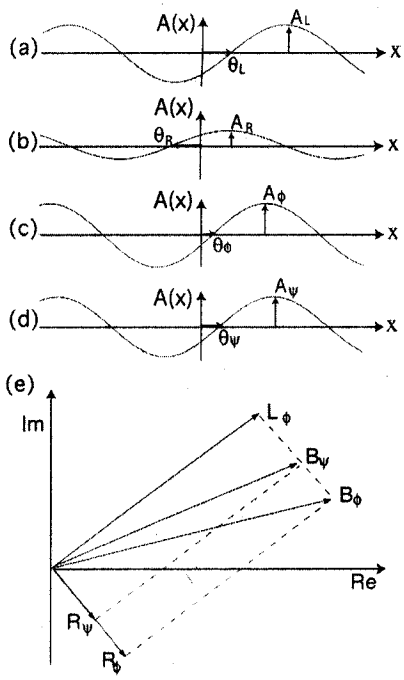


Figure 15.1. Vector presentations of sine waves and their arithmetic summation in the complex plane. (a) Representation of a horizontal sinewave grating presented to the left eye with modulation amplitude $A_L$ and phase $\theta_L$. The abscissa represents the vertical direction $x$ and the ordinate is amplitude $A(x)$. (b) A horizontal grating presented to the right eye with modulation amplitude $A_R$ and phase $\theta_R$. (c) The physical, algebraic sum of gratings (a) and (b) has modulation amplitude $A_\phi$ and phase $\theta_\phi$. (d) The (perceived) cyclopean grating has modulation amplitude $A_\psi$ and phase $\theta_\psi$. (e) The complex plane. The abscissa is the real axis and the ordinate is the imaginary axis. Vector $\vec{L}_\phi$ and vector $\vec{R}_\phi$ represent the sine waves presented to the left and right eyes, respectively. The vector components of $\vec{L}_\phi$, ($A_L$, $\theta_L$), are shown as vectors (arrows) in (a). Other vectors in (e) are similarly derived from the components shown in (b, c, d). Vector $\vec{B}_\phi$ is the vector sum: $\vec{B}_\phi$=$\vec{L}_\phi$+$\vec{R}_\phi$. Vector $\vec{B}_\psi$ is drawn with a phase angle that represents the psychophysically measured phase of the (perceived) cyclopean sine wave. Vector $\vec{R}_\psi$ represents a reduced right-eye contribution to the cyclopean sine wave that would account for the (perceived) cycopean phase.

sine waves. It is both reasonable to assume and empirically observed that the cyclopean image of two parallel monocular sinewave gratings of the same wavelength is indeed, to a very close approximation, a sinewave grating of the same wavelength. Therefore, in this instance, predicting the combined cyclopean image is equivalent to predicting the apparent phase and amplitude of the cyclopean sinewave grating.

Consider two monocular images, parallel sinewave gratings, that differ in phase

and amplitude. If the binocular combination were linear, the apparent phase of the cyclopean sinewave grating would be predicted by a simple vector summation of the monocular sine waves. Our experimental results indicate that the apparent phase of the cyclopean sinewave grating, relative to vector summation, is biased toward the eye with the higher-contrast stimulus. For example, in Figure 15.1, the left eye is presented with a higher-contrast sinewave grating $\vec{L}_\phi$ and the right eye with a lower-contrast sinewave grating $\vec{R}_\phi$. Linear vector summation is $\vec{B}_\phi = \vec{L}_\phi + \vec{R}_\phi$. The observed cyclopean image is $\vec{B}_\psi$, which is biased toward the left (higher-contrast) eye relative to vector summation.

**Binocular combination implies attenuation of a weaker signal relative to a stronger signal**

We interpret the observed failure of vector summation in predicting cyclopean images by assuming: (1) there is vector summation of left- and right-eye same-wavelength sinewave gratings and (2) prior to the site of binocular combination, the physically weaker (lower contrast) monocular image is attenuated relative to the stronger (higher-contrast) monocular image. In the example of Figure 15.1, if the physical right monocular image ($\vec{R}_\phi$) were attenuated to precisely $\vec{R}_\psi$, it would reproduce precisely the experimentally observed cyclopean phase. The contrasts of the physical stimuli are in a ratio of 2:1; the observer acts as though the ratio were 4:1. This assumed perceptual attenuation of the lower-contrast relative to the higher-contrast monocular grating is the critical derived measurement that we subsequently use to construct our theory of binocular combination.

**Outline**

In this chapter, we offer a procedure for measuring the apparent phase of a cyclopean sinewave grating. The observer's task is to judge the center position of the black stripe that corresponds to the minimum in the cyclopean sinewave grating relative to the position of an adjacent reference line. We present a gain-control model to fit our data. The model accounts for over 97% of the variance of the experimental data in the sense of successfully predicting the apparent phase of the cyclopean sinewave grating. In our experiments, we measure only the phase, not amplitude of the cyclopean sine wave. To determine whether the model can predict amplitude as well as phase, we rely on the contrast-matching data of Legge and Rubin (1981). By means of model simulations, we find that the model does indeed give a united explanation of binocular combination data derived from simple stimuli. The model does not deal with complex binocular combinations that involve faces and other meaningful stimuli (see Blake, 2003) in which higher-order visual processes are probably involved.

## 15.1.2 Empirical manipulations in the sinewave summation experiments

Figure 15.2 outlines the principles used to derive the relative contribution of the left- and right-eye images to the cyclopean image. Basically, given the physically presented

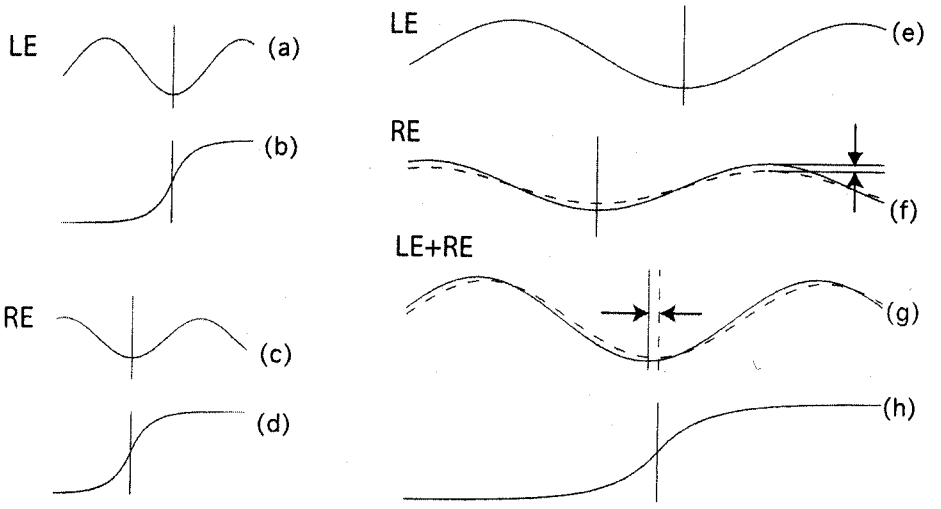


Figure 15.2. Control conditions, experimental conditions, and their interpretations. (a, c) Only one eye is presented with a sinewave grating (as illustrated). (b,d) Psychometric functions. The fraction of trials on which the reference lines are judged above the dark stripe of the sinewave grating as a function of the vertical position of the reference lines. The midpoint of a psychometric function (indicated by the vertical bar) is taken as the perceived phase of the presented sinewave. The right column shows binocular conditions. The scale is magnified to better illustrate the results. (e) A high-contrast sine wave presented to the left eye (LE). The solid vertical line indicates the midpoint of the dark stripe. (f) The solid curve represents a low-contrast sine wave presented to the right eye (RE). (g) The algebraic sum of (e) and (f) is shown as a solid line. (h) The perceived phase of cyclopean sine wave is measured by a psychometric function. It is closer to the phase of the left eye's stimulus than would be expected from the algebraic sum (g). An attenuated lower-contrast sine wave is shown as a dotted line in (f). Using this attentuated lower-contrast sine wave to form the left-plus-right-eye sum (dashed line in (g)) causes the algebraic sum of the original left-eye sinewave and the attentuated right-eye sine wave to match the phase of the cyclopean sine wave. The change from physical contrast of the stimulus to effective contrast at the point of binocular combination is here expressed as a reduction in effectiveness of the lower-contrast sinewave grating. However, for a given pair of left- and right-eye sinewave grating phases, the phase of the cyclopean sine wave is determined entirely by the *ratio* of left- to right-eye effective contrasts.

phases of the two monocular stimuli, and the phase of the perceived cyclopean image, we calculated the attenuation of the lower-contrast stimulus that would be required to reproduce the observed cyclopean phase. In control conditions, on each trial only one randomly chosen eye was presented with a sinewave grating. The other eye was simultaneously presented a blank screen with the same mean luminance as the sinewave grating. These control stimuli were interleaved in a sequence of experimental displays.

Indeed, observers could not distinguish control from experimental conditions, and were unaware that occasionally only one eye had received a grating stimulus.

**Psychometric functions**

To measure a psychometric function, the position of the reference line relative to the sine wave was varied from trial to trial using a staircase procedure described below. On each trial, the observer judged whether the reference line was "above" or "below" the center of the black stripe in the cyclopean sinewave grating. The position of the reference line that was equally likely to be judged as "above" and "below" was taken as the Point of Subjective Equality (PSE), i.e. the median perceived position of the center of the black stripe of the cyclopean sinewave grating.

Figures 15.2 a-d illustrate the control trials. Figure 15.2a illustrates the stimulus for control trials with a left-eye stimulus, and Figure 15.2c illustrates the right-eye stimulus. Figures 15.2 b,d illustrate psychometric functions derived from presentations of these stimuli and the estimated positions of the PSEs. Typically, the measured value of apparent phase $\hat{\theta}_L$ of the PSE differed slightly but significantly from the physical value of $\theta_L$, indicating a small bias of the measurement. When two psychometric functions for $\hat{\theta}_R$ and $\hat{\theta}_L$ are obtained in the same session, the position bias would be expected to be the same and therefore canceled by considering the difference $\hat{\theta}_L - \hat{\theta}_R$. The phase difference between the perceived phases of the left- and right-eye control sine stimuli would be expected to be identical to the phase difference between the input sines, i.e. $\hat{\theta}_L - \hat{\theta}_R = \theta_L - \theta_R$. Satisfaction of this constraint within a small measurement error was verified for each observer before each experimental session.

In experimental sessions, staircases for control conditions were interleaved with the staircases for measurement conditions. As noted above, observers did not discriminate monocular from binocular trials. In experimental trials, observers view sinewave gratings that might differ between eyes in both spatial phase and contrast. Figures 15.2e and f illustrate stimuli in which the left eye was presented with a higher-contrast sinewave grating with phase $\theta_L$ (Figure 15.2e) and the right eye was presented a lower-contrast sinewave grating with phase $\theta_R$ (Figure 15.2f). The linear summation of these two sine waves is again a sine wave, illustrated by the solid line of Figure 15.2g. The location of its minimum is indicated by a solid vertical line.

The perceived binocular combination of the left- and right-eye's gratings, the cyclopean image, is assumed to be a sinewave grating whose apparent phase is measured by a psychometric function (Figure 15.2h). To arrive at an arithmetic summation of the left and right eyes' sinewave gratings that has the same phase as the cyclopean sinewave grating, we assume that the signal from the right eye (the lower-contrast stimulus) was attenuated prior to binocular combination. This assumed-attenuated right-eye input to binocular combination is shown by the dashed line in Figure 15.2f. The combination of the unattenuated higher-contrast input and the attenuated lower-contrast input is illustrated by the dashed line in Figure 15.2g. The minimum of this combination now precisely matches the observed position derived from the emprical psychometric function Figure 15.2h.

Many observers exhibit some eye dominance. That is, in binocular combination, the input from one eye (the dominant eye) is given greater weight than that from the

other eye. To cancel biases of measurement related to eye dominance, the experiment was repeated with the stimuli to the two eyes interchanged. The average of these two measured phase shifts was taken as the phase shift for the cyclopean condition. Additionally, to cancel biases related to vertical position, all the above procedures were repeated with the stimuli mirror-reflected around the horizontal midline, and all the results were averaged.

### 15.1.3 Outline of the experiments

Six experiments were performed. In all experiments, observers judged the vertical position (phase) of a horizontal sinewave grating that was presented to both eyes. In experiment 1, no external noise or mask was superimposed and simple sinewave gratings were presented to the left and right eyes in various different phases and with various different contrasts. The data of experiment 1 are accounted for by the gain-control model described below with just one free parameter.

Experiment 2 investigated the prediction that reducing contrast energy reduces the nonlinearity of (i.e. linearizes) binocular combination. The stimuli and procedure were similar to experiment 1 except the fixed duration of 1000 ms in experiment 1 was varied in the range from 50 ms to 1000 ms, creating stimuli ranging from very low contrast energy (50 ms $\times$ 0.1) to very high energy (1000 ms $\times$ 0.2). This experiment defines the temporal parameters of interocular gain control in binocular combination.

Experiments 3–6 measured the gain-control factors that determine binocular dominance. In these experiments, a monocular masking stimulus was superimposed on the sinewave gratings whose phase was being judged. Experiment 3 investigated the question: When the spatial frequency for which binocular combination is being determined is $f_0$, how much do other spatial frequencies $f_1$ contribute to gain control? This was tested by superimposing a 2D bandpass noise on the sinewave grating in just one of the two eyes.

In experiment 4, a static vertical sinewave grating was used to mask the horizontal sinewaves whose position was being judged. The contrast and spatial frequency of the masking grating was varied from trial to trial. Spatial-frequency transfer functions were obtained.

In experiment 5, the binocular horizontal grating whose position was being judged was masked by a monocular moving vertical sinewave grating whose contrast and drift rate vary from trial to trial. Temporal-frequency transfer functions were obtained.

In experiment 6, the orientation of a static, sinewave masking grating was varied. Orientation tuning functions were obtained.

## 15.2 Methods

### 15.2.1 Apparatus

The purpose of the apparatus was to produce a binocular display in which each eye is presented with a horizontal sinewave grating, and the two eyes' images are optically superimposed. The two sinewave gratings are identical except for differences in phase

and contrast. The reason for choosing sine waves is that the sum of two sine waves of the same wavelength is again a sine wave. Typically, for the parameters used in the experiments of this paper, the observer perceived a cyclopean sinewave grating. Sinewave gratings were horizontal to make the cyclopean image relatively independent of horizontal vergence angle. A high-contrast surrounding visual frame was used to assist the eyes in maintaining vergence. The task of the observer was to judge the position of the center of the dark stripe of the cyclopean sinewave gratings relative to two adjacent dark reference lines.

### 15.2.2 Display

The experiments were controlled by an 8600/250 Power Macintosh; stimuli were presented on a Nanao Technology monochrome monitor. The programs were written in Matlab, using the Psychophysics Toolbox extensions (Brainard, 1997; Pelli, 1997). A special circuit (Pelli and Zhang, 1991) was used to combine two eight-bit output channels of the video card to yield 6144 distinct gray-scale levels (12.6 bits). The luminance of the monitor with all pixels set to the minimum value was 0.38 cd/m$^2$; the luminance with all pixels set to the maximum value was 68.1 cd/m$^2$. The background level $I_0$ surrounding the sinewave gratings was set to 34.2 cd/m$^2$, and this was also used as the average luminance of the sine waves themselves. Displays were viewed in a mirror stereoscope and positioned optically 68 cm from the observer.

A psychophysical procedure was used to generate a linear look-up table. This look-up table was used, as required, in either of two ways: (1) to divide the entire dynamic range of the monitor into 256 evenly-spaced gray levels or (2) to select 256 evenly-spaced grey levels within a limited intensity range and thereby to obtain higher contrast resolution within that range (Lu and Sperling, 1999).

### 15.2.3 Stimuli

Horizontal gratings with sinusoidal luminance profiles were used as stimuli. To describe these stimuli we make the following definitions: $I_0$ is luminance of the background and the mean luminance of the sinewave gratings; $m_{\text{L}}$ and $m_{\text{R}}$ are the modulation contrasts of the left- and right-eye sinewave gratings, respectively; $\theta_{\text{L}}$ and $\theta_{\text{R}}$ are the corresponding phases. In experiments 3–6, a mask $\mathcal{M}(x, y)$ which consisted of either a bandpass noise or a sinewave grating was superimposed on the sinewave grating presented to one eye. The mask's modulation contrast is either $n_{\text{L}}$ or $n_{\text{R}}$ corresponding to adding the mask either to left or to right eye. The stimuli were windowed in a rectangular window both spatially and temporally. Equations (15.1) and (15.2) describe the stimuli to the left and right eyes respectively,

$$I_{\text{L}} = I_0 - (m_{\text{L}} \cos(2\pi f_s x + \theta_{\text{L}}) + n_{\text{L}}\mathcal{M}(x, y))I_0 u(t, T)u(x + 2\pi, 4\pi)u(y + 2\pi, 4\pi) \tag{15.1}$$

$$I_{\text{R}} = I_0 - (m_{\text{R}} \cos(2\pi f_s x + \theta_{\text{R}}) + n_{\text{R}}\mathcal{M}(x, y))I_0 u(t, T)u(x + 2\pi, 4\pi)u(y + 2\pi, 4\pi). \tag{15.2}$$

Stimuli appeared for a duration $T$ defined as follows:

$$u(t,T) = \begin{cases} 1 & \text{if } 0 \le t \le T \\ 0 & \text{otherwise} \end{cases} . \tag{15.3}$$

In experiment 2, $T$ varied from 50 ms to 1000 ms; in all other experiments, $T$ was fixed at 1000 ms. In experiments 1 and 2, no mask was superimposed, i.e., $n_L = n_R = 0$. In all trials for all experiments, the spatial frequency of the gratings $f_s$ was fixed at 0.68 cpd and there were exactly two cycles ($4\pi$) visible in each eye's sinewave grating. A reference line was shown on each side of the sinewave grating. A high-contrast, surrounding visual frame was presented from the start of the trial until the end of the stimulus presentation to assist observers in maintaining vergence (Figure 15.3).

### 15.2.4 Procedures: Sequence of events on a trial

Figure 15.3 shows the procedures used in experiment 1. The two left-hand columns show the stimuli presented to the left and the right eyes respectively. The right-hand column represents the cyclopean image perceived by an observer. Every trial began with two fixation crosses, each with two dots, presented to two eyes and arranged so that with correct vergence, a single cross with four symmetrically placed dots would be perceived (Figure 15.3a). Only after this cross with four symmetric dots was seen clearly, did the observer press a key to initiate the trial. The key press produced a screen with only the high-contrast frame (Figure 15.3b) for 500 ms followed by sinewave gratings presented to the two eyes for one second (Figure 15.3c). Stimulus presentation was followed by a blank screen of mean luminance until the observer responded.

The observer's task was to indicate the apparent location of the center of the dark stripe in the perceived cyclopean sinewave grating relative to a black horizontal reference line adjacent to its edge. If the reference line were judged above the dark cyclopean stripe, a key press indicating "above" was made; if the line were judged below, the "below" key press was made. After the response, the preparation for the next trial began with presentation of the cross-plus-dots fixation images.

In experiments 3–6, the procedures were exactly the same as that in experiment 1 except that a masking bandpass noise or a masking sinewave grating was randomly superimposed on one eye's sinewave grating.

### 15.2.5 Procedures: Adaptive concurrent staircases

An adaptive staircase procedure, with many concurrent staircases, was used in all experiments. Within a staircase, the position of the reference line was varied according to the response in the previous trial of that staircase. In each staircase, when the response was "Above," the reference line was moved down on the next trial of that staircase; when the response was "Below," the reference line was moved up in the next trial. For each condition, four staircases were interleaved randomly, corresponding to the four variations of each experimental condition: the higher-contrast sinewave grating presented either to the left or right eye with either the original display or a mirror reflection of the origial display around the horizontal midline. For an experiment with $n$

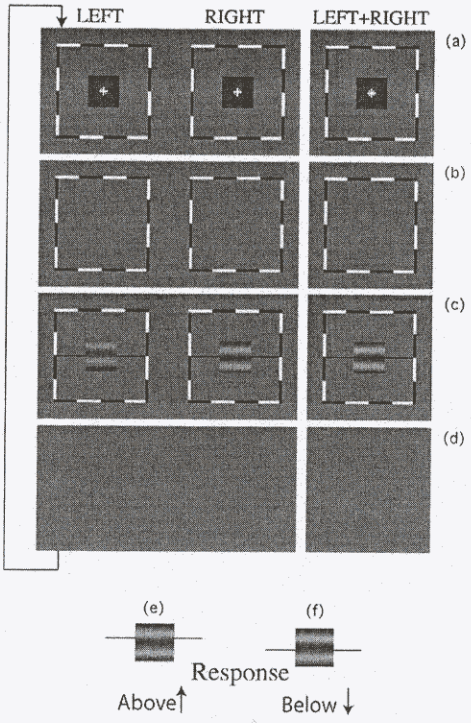


Figure 15.3. Procedure used in Experiments 1, 3, 4, 5, and 6. The column "LEFT" shows the stimuli presented to the left eye; the column "RIGHT" shows the stimuli presented to the right eye; the column "LEFT+RIGHT" illustrates the arithmetic sum of these stimuli. (a) A cross-hair with two dots was presented to each eye; when the eyes were correctly verged, a cyclopean cross with four dots was perceived. (b) Once vergence has been achieved, a key is pressed that changes the stimulus to a blank field (with only the surrounding frame) for 500 ms. (c) Horizontal sinewave gratings were presented to each eye for 1000 ms. Black horizontal reference lines were adjacent to the edges of the gratings. The cyclopean image was also a sinewave in which the observer judged the position of the reference line relative to the center of the central dark stripe of the grating. In experiment 3, a bandpass noise is added to one of the sinewave gratings in one eye; in experiments 4, 5 and 6, a masking sine wave was added to one eye's sinewave gratings. (d) A blank screen persisted until a response was made. (e) A cyclopean image for a response "reference line above dark stripe." (f) A cyclopean image for a response "reference line below dark stripe." After the response, the entire sequence repeated.

conditions, $4n$ staircases were run concurrently and interleaved randomly. Each staircase was run for a total of 50 trials.

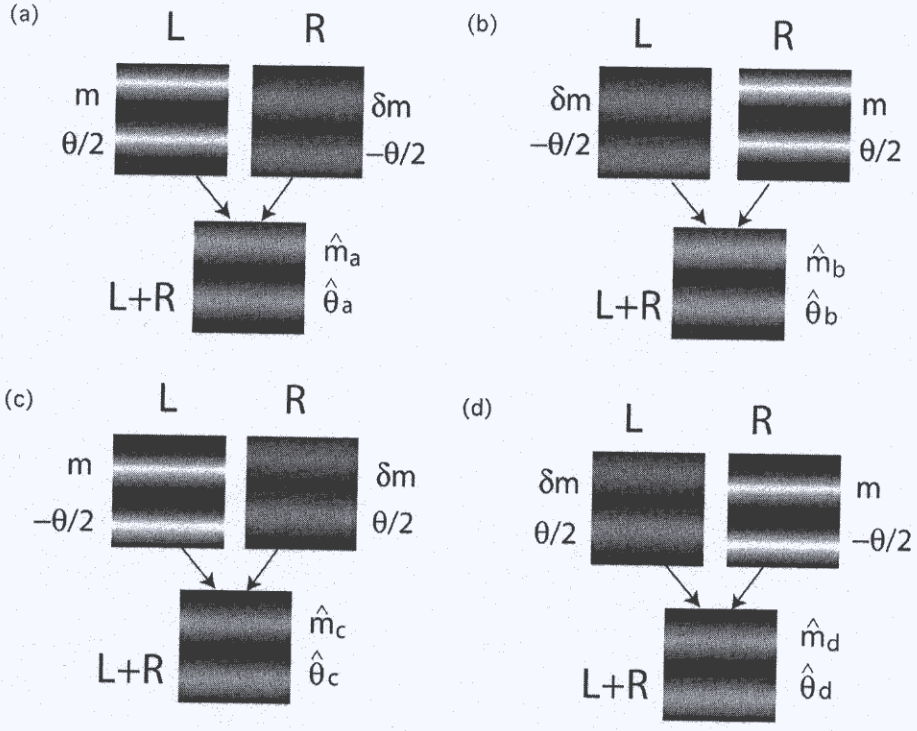


$$\hat{\theta} = \frac{\hat{\theta}_a + \hat{\theta}_b}{2} - \frac{\hat{\theta}_c + \hat{\theta}_d}{2}$$

Figure 15.4. The four binocular stimuli used to cancel position and eye biases and thereby to yield unbiased estimates of the perceived phase of cyclopean images produced by left-eye (L) and right-eye (R) gratings that differ in contrast by a factor of $\delta$ and in phase by $\theta$. (a, L) High-contrast grating with modulation amplitude m in the left eye and with dark band $\theta/2$ above the midline. (a, R) A low-contrast grating with modulation $\delta$m, $0 \leq \delta \leq 1$, and with the dark band below the midline presented to the right eye. The cyclopean image perceived when L+R are presented has perceived contrast $\hat{m}_a$ and perceived phase $\hat{\theta}_a$. (b) High-contrast m in right eye, dark stripe $\theta/2$ (above midline). (c) High-contrast m in left eye, dark stripe $-\theta/2$ (below midline). (d) High-contrast m in right eye, dark stripe $-\theta/2$ (below midline). The estimated cyclopean phase shift $\hat{\theta}$ produced by left-eye and right-eye gratings that differed in contrast by $\delta$ and phase by $\theta$ is given by the formula at the bottom. Note that whenever $\delta = 1$, the expected value of $\hat{\theta} = 0$; whenever $\delta = 0$, the expected value of $\hat{\theta} = \theta$.

### 15.2.6 Procedures: Counterbalancing to control for eye and position biases

The basic stimuli used in all experiments are described by Eqs. (15.1) and (15.2) and Figure 15.3. A horizontal sinewave was presented to each eye. The contrast of the higher-contrast sinewave grating was $m$, the contrast of the lower-contrast sinewave grating was $\delta m$, where $0 \leq \delta \leq 1$. The phase difference between the left- and right-eye sinewave gratings was $\theta$. For any given combination of $m$, $\delta$, $\theta$ there were four alternative stimuli: The higher-contrast sinewave grating could be presented either to the left (Figures 15.4a and c) or to the right (Figures 15.4b and d) eye and the higher contrast can be assigned to either the upper (Figures 15.4a and b) or to the lower (Figures 15.4c and d) sinewave grating in the combination (causing the dark stripe to appear either above or below the midline).

For any condition (a combination of $m$, $\delta$, $\theta$) four independent staircases corresponding to the four configurations of Figure 15.4 were conducted. The four staircases for each condition were combined (see below) to give a single-valued dependent variable: the perceived phase shift between applying the higher contrast to the upper versus to the lower sine wave in the combination. This measure cancelled modest dominance biases in favor of one or the other eye, and perfectly cancelled up/down location biases in judging the position of the center of the cyclopean grating's dark band relative to the reference lines.

Figure 15.5 shows an example of how we measured the perceived phase shift for the following condition: $m = 10\%$, $\theta = 90°$, and $\delta = 0.5$ (i.e. the contrast of the higher-contrast sinewave grating was 10%, that of the lower-contrast sinewave grating was 5%). In viewing these stimuli, observers generally were unaware of having gratings of different contrast in each eye; they perceived only a cyclopean grating.

There were four alternative sine wave presentations of this combination of parameters, in each of which the dark band of one sine wave was 45° above the midline and the dark band of the other was 45° below the midline:

(*a*) The 10% grating was presented to the left eye and its dark band was the higher of the two sinewave components (Figure 15.4a), i.e. $m_L = 10\%$, $\theta_L = 45°$, $m_R = 5\%$ and $\theta_R = -45°$.

(*b*) The 10% grating was presented to the right eye and its dark band was the higher of the two sinewave components (Figure 15.4b), i.e. $m_L = 5\%$, $\theta_L = -45°$, $m_R = 10\%$ and $\theta_R = 45°$.

(*c*) The 10% grating was presented to the left eye and its dark band was the lower of the two sinewave components (Figure 15.4c), i.e. $m_L = 10\%$, $\theta_L = -45°$, $m_R = 5\%$ and $\theta_R = 45°$.

(*d*) The 10% grating was presented to the right eye and its dark band was the lower of the two sinewave components (Figure 15.4d), i.e. $m_L = 5\%$, $\theta_L = 45°$, $m_R = 10\%$ and $\theta_R = -45°$.

Let $\hat{\theta}_i$ be the perceived position of the dark stripe of the cyclopean sinewave in condition $i$ ($i = a, b, c, d$). Then: $(\hat{\theta}_a + \hat{\theta}_c)/2$ and $(\hat{\theta}_b + \hat{\theta}_d)/2$ are measures of position bias; $\hat{\theta}_b - \hat{\theta}_a$ and $\hat{\theta}_d - \hat{\theta}_c$ are measures of eye bias; and $\hat{\theta}_a - \hat{\theta}_c$ and $\hat{\theta}_b - \hat{\theta}_d$ are left- and right-eye measures of a phase shift induced by unequal left- and right-eye grating

contrasts. The left- and right-eye measures of phase shift can be combined into a single quantity, the perceived phase shift:

$$\hat{\theta} = \frac{\hat{\theta}_a + \hat{\theta}_b}{2} - \frac{\hat{\theta}_c + \hat{\theta}_d}{2}. \tag{15.4}$$

The perceived phase shift $\hat{\theta}$ has the useful property that, except for measurement error, when $\delta = 1$, $\hat{\theta} = 0$; when $\delta = 0$, $\hat{\theta} = \theta$. The perceived phase shift $\hat{\theta}$ is the dependent variable in all the experiments.

As shown in Figure 15.5, for a given condition of $m$, $\delta$, and $\theta$, each $\hat{\theta}_i$ ($i$ = a, b, c, d) was first measured by the corresponding psychometric function, and then the perceived phase shift $\hat{\theta}$ was calculated by Eq. (15.4).

### 15.2.7 Observers

Three observers were tested, the first author and two naïve observers, one of whom only participated in experiment 1. All had normal or corrected-to-normal vision.

## 15.3 Experiment 1. Binocular combination as determined by the interocular contrast ratio, the interocular grating phase difference, and overall contrast level

Experiment 1 measured the influence of the absolute contrast, relative contrast, and the relative phase of gratings in the left and right eyes on the cyclopean image.

### 15.3.1 Stimuli

The independent variables in the experiment were the contrast of the higher-contrast sinewave grating, $m = \max\{m_L, m_R\}$, the contrast of the lower-contrast sinewave grating which is expressed as a contrast ratio of lower/higher, $\delta = \min\{m_L, m_R\}/\max\{m_L, m_R\}$, and the phase difference, $\theta = \max\{\theta_L, \theta_R\} - \min\{\theta_L, \theta_R\}$, between the sinewave gratings presented to the left and right eyes. The duration of the stimulus $T$ was fixed at 1000 ms.

### 15.3.2 Psychometric functions

The data are displayed as psychometric functions: the fraction of trials (converted to a probit) in which the reference line was judged to be above the middle of the dark band of the grating is plotted as a function of the vertical position of the reference line. Figure 15.5 illustrates four psychometric functions corresponding to four variations $a$, $b$, $c$ and $d$ (see also Figure 15.4) at a condition of $m = 10\%$, $\delta = 0.5$ and $\theta = 90$ for a single observer. In each plot, the abscissa is the position of the reference line in phase degrees relative to the center of the frame. The ordinate is the fraction of trials

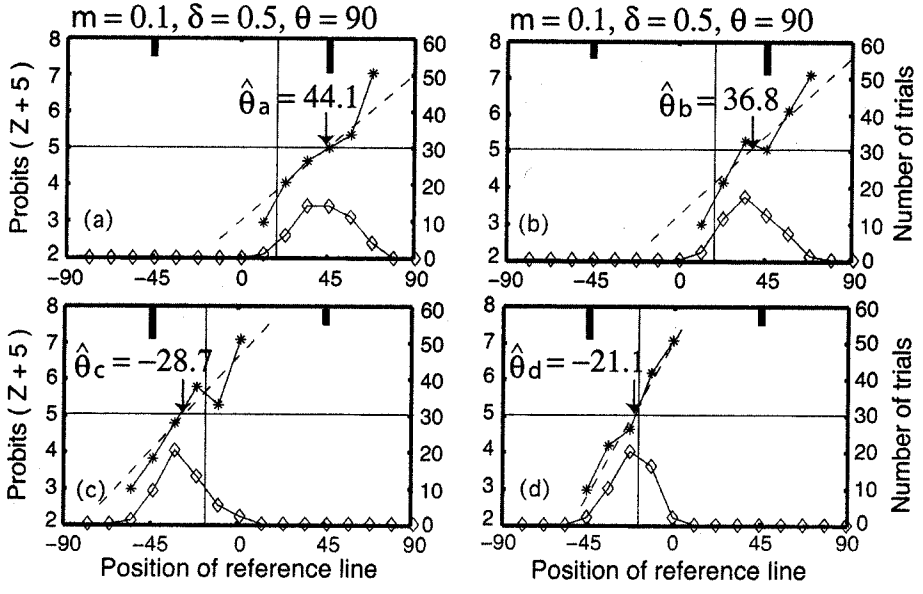


$$\hat{\theta} = \frac{\hat{\theta}_a + \hat{\theta}_b}{2} - \frac{\hat{\theta}_c + \hat{\theta}_d}{2} = 65.4$$

Figure 15.5. Psychometric functions and probit analyses. The data illustrated in panels (a), (b), (c), (d) correspond to the stimulus configurations (a), (b), (c), (d) of Figure 15.4. The left- and right-eye stimuli themselves are represented as bars at the top edge of the figure at $-45°$ and $+45°$, the length of the bar indicates the relative contrast. The abscissa is the position of the reference line measured in phase degrees of the sinewave grating; the ordinate is the fraction of trials on which the reference line was judged as being above the black stripe measured in probits (probits = Zscore + 5). Five probits corresponds to 50% probability. The bell-shaped curves at the bottom of the figure represent the number of trials actually conducted at the indicated position of the reference line; the right-hand ordinate indicates the number of trials. The dashed lines are maximum likelihood best fits (assuming Gaussian distributions) to the psychometric function data; their intersection with the horizontal 50% line represents the estimated cyclopean phase $\hat{\theta}_i$, i = $a$, $b$, $c$, $d$. The vertical lines represent predictions based on algebraic (linear) addition of the left- and right-eye stimuli and indicate a phase shift $\hat{\theta}_{linear}$ of 36° owing to unequal contrasts in the two eyes compared to the empirically observed phase shift of $\hat{\theta}$ of 65.4°.

(converted to probits) on which the reference line was judged to be above the center of the dark band of the cyclopean grating. The ordinate is shown as probits (inverse normal density function, probits = Zscore + 5) so that if measurement errors were normally distributed, the data would fall on a straight line. Five probits corresponds to 50% probability.

Probits analysis (Finney, 1971) was used to fit the data. The slanted dashed line is the best-fitting straight line. The staircase procedure generated the most trials near 5 probits, and therefore these data have the most weight in the Maximum Likelihood Estimation of the best fit. The actual number of trials at each position of the reference line is illustrated at the bottom of each plot; the right-hand ordinate indicates the number of trials.

The apparent phase of the cyclopean grating is defined as the point at which the reference line is equally likely to be judged above and below the center of the dark band, i.e., the abscissa value at 5 probits, which we designate as $\hat{\theta}_i$ ($i = a, b, c, d$). The best-fitting straight line was determined by probit analysis. In the example of Figure 15.5a, the center of the dark band was judged to be higher above the center of the display, $\hat{\theta}_a = 44.1°$. The same analysis was applied to the data of conditions $b$, $c$ and $d$ (Figures 15.5b, c, and d, respectively), in which the apparent center of the dark band was judged to be at $\hat{\theta}_b = 36.8°$, $\hat{\theta}_c = -28.7°$, and $\hat{\theta}_d = -21.1°$, respectively.

Measurements $\hat{\theta}_a$, $\hat{\theta}_b$, $\hat{\theta}_c$, and $\hat{\theta}_d$ of the apparent phase shift tended to be biased slightly upwards. Whether this was due to a bias in the visual system, or due to the way pixels were designated in the display is immaterial because this bias is cancelled by considering only the difference given in Eq. (15.4), and never $\hat{\theta}_i$ ($i = a, b, c, d$) individually. The perceived phase shift $\hat{\theta}$ has two noteworthy properties: When there was no contrast difference between the left- and right-eye gratings, the displays of Figure 15.4a and Figure 15.4d are physically identical, as are the displays of Figure 15.4c and Figure 15.4b; therefore, the expected value of $\hat{\theta}$ is zero. When the lower-contrast grating has a contrast of zero, so that only the higher-contrast grating is visible, the expected value of $\hat{\theta}$ is simply the phase difference $\theta$ between the left- and right-eye gratings ($\theta = \theta_L - \theta_R = 90°$ in the example of Figure 15.5). The perceived phase shift $\hat{\theta}$ (Eq. (15.4)) measures how far a particular contrast ratio $\delta$ pushes the cyclopean perception $\hat{\theta}$ towards the maximum possible value $\theta$ (which is achieved when the left- and right-eye grating contrasts, respectively, are 1 and 0 ($\delta = 0$)).

The solid vertical lines in the plots of psychometric function (Figure 15.5) indicate the locations of the centers of the dark bands predicted by linear summation of the left- and right-eye images. The measured locations of the cyclopean gratings were more shifted toward the higher-contrast grating than predicted by simple linear addition of left- and right-eye inputs. This would occur if the linear prediction over-estimated the relative contribution of the lower-contrast grating to the cyclopean perception, i.e. if the effective $\hat{\delta}$ in this example were less than the the actual $\delta$ of 0.5.

### 15.3.3 Control conditions

We consider here the control conditions for experiment 1 in which the phase difference $\theta$ between the left- and right-eye sine waves was 90°. In the first set of control conditions, only one eye was presented with a sinewave grating, i.e. $\delta = 0$. This sinewave grating could be 45° above the midline in the left or right eye (conditions a and b, Figures 15.4a and 15.4b), or 45° below the midline (conditions c and d, Figures 15.4c and 15.4d). The perceived phase shift, $\hat{\theta}$ from Eq. (15.4), of cyclopean sinewave gratings should be the same as the actual phase difference $\theta$ of the input sinewave gratings, i.e. $\hat{\theta} = \theta = 90°$. Position bias can be evaluated in each control condition individually; it

cancels in the difference.

In a second set of control conditions, the two eyes were presented with sinewave gratings of exactly the same contrast, i.e., $\delta = 1$. In this case, conditions $a$ and $d$ (as described above) were identical, as were conditions $c$ and $b$. There would be a perceived difference between conditions $a$ and $b$ (left eye sinewave grating below or above midline) only if the left and right eyes did not have equal weight. For example, if the left eye was strongly dominant, then moving the dark band from above the midline to below the midline in the right eye (from $a$ to $b$) would produce a big change in apparent position of the band. On the other hand, if the two eyes were equal in dominance, then there would be no perceived change. So, the subtraction (b + c) minus (a + d) gives an indication of the degree of difference in weights given to the left- and right-eye images.

Before formal data collection in an experiment session began, a preliminary session including two control conditions of $\delta = 0$ and $\delta = 1$ was carried out to evaluate position bias and ocular dominance. In fact, none of the three observers showed significant ocular dominance as tested with these sinewave gratings.

### 15.3.4 Results

Figure 15.6 shows the results of experiment 1. The data are the $\hat{\theta}$ values representing the perceived phase shift of cyclopean stimuli in which the dark band of the cyclopean sinewave grating (determined by the higher-contrast sine wave) was set above and below the midline position. The four different types of trials used to collect such a difference cancel linear components of position and eye bias. The contrast of the higher-contrast grating $m$ took the following values, each of which is represented in an individual panel of Figure 15.6: (a) 5%, (b) 10%, (c) 20%, and (d) 40%. The phase difference $\theta$ took the values 45° (+), 90° (∗) and 135° (×), and the contrast ratio $\delta$ varied among 0.3, 0.5, 0.71, and 0.86 (abscissa). The ordinate is the perceived phase shift $\hat{\theta}$ produced by the asymmetry of the stimuli in the two eyes (see Eq. (15.4)). The dashed curves are predictions of the linear summation model. Linear summation gave a poor fit to the results except in the control conditions for which the predictions are trivial. In Figure 15.6, the solid lines are one-parameter fits to the data generated by the gain-control model described later in this article. Figures 15.7 and 15.8 show data for two additional observers.

All the data for all the observers lie above the linear prediction. This means that when the input contrasts to the two eyes are unequal, the higher-contrast grating has more weight (relative to the lower-contrast grating) in determining the cyclopean grating than predicted by linear summation of the inputs to the two eyes. In other words, the effective interocular contrast ratio $\hat{\delta}$, which can be calculated from the perceived phase shift $\hat{\theta}$, was smaller than the real contrast ratio. Figure 15.9 shows the effective interocular contrast ratio $\hat{\delta}$ as a function of the real contrast ratio $\delta$ in a log-log graph. The data are illustrated by lower-case letters that represent the experimental conditions. The dashed line is $\hat{\delta} = \delta$, the prediction of linear summation. The solid line with slope $1+\gamma$ is $\hat{\delta} = \delta^{1+\gamma}$, the prediction of the gain-control model with best fitting $\gamma$ from Figures 15.6, 15.7 and 15.8 for each observer. The greater spread of data for small $\delta$ is due to the fact that the variance of position judgements is relatively constant, independent of $\delta$. Therefore the variance in $\log \hat{\delta}$ is proportional to $-\log(\delta)$.

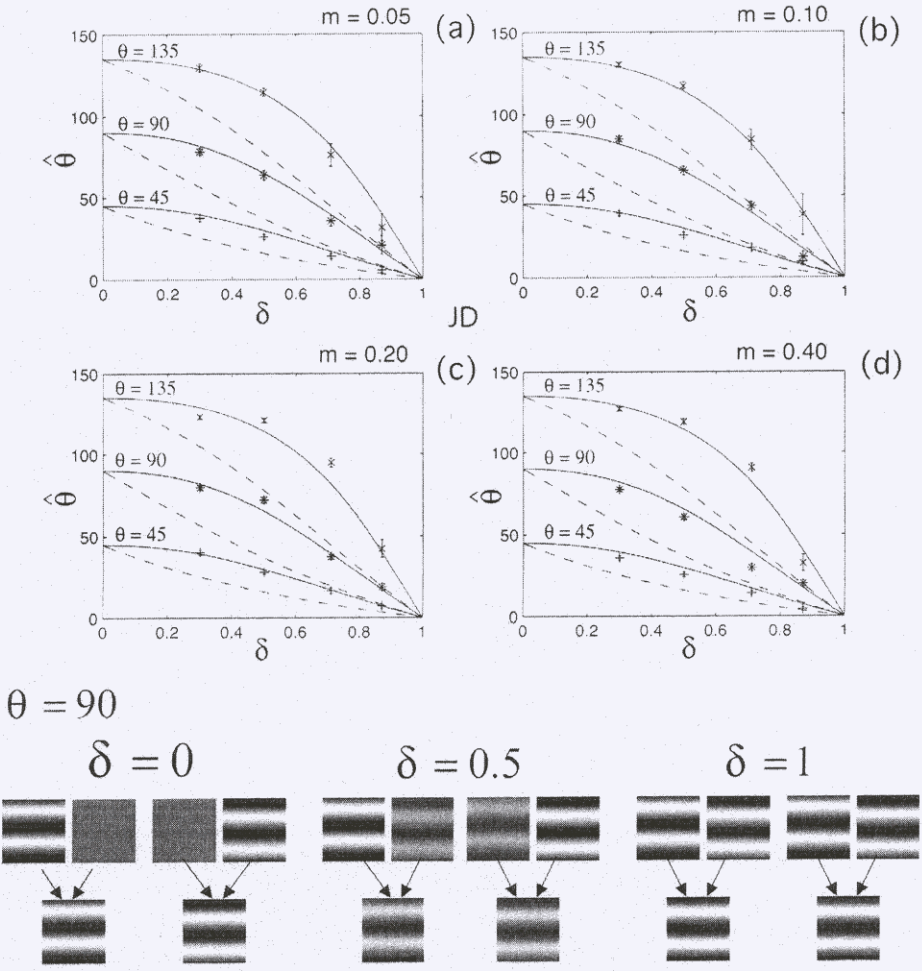


Figure 15.6. Results of experiment 1. How the interocular contrast ratio affects binocular combination: Perceived phase shift $\hat{\theta}$ as a function of the interocular contrast ratio for three phase differences of the interocular gratings and for four contrasts of the higher-contrast grating. Each panel shows the perceived phase shift $\hat{\theta}$ as a function of contrast ratio $\delta$ when the interocular grating phase difference $\theta$ is 45° (+), 90° (∗), or 135° (×), and the greater contrast $m$ was (a) 5%, (b) 10%, (c) 20%, or (d) 40%. The stimulus duration $T$ was fixed at 1000 ms. The abscissa is the interocular contrast ratio $\delta$; the ordinate is the measured cyclopean phase shift $\hat{\theta}$. The solid lines are best fits of the gain-control model (see below); the dashed lines are predictions of algebraic (linear) summation of the left- and right-eye stimuli. Inserts at the bottom show left- and right-eye stimuli together with the cyclopean (perceived) images for three contrast ratios $\delta$ with an interocular grating phase difference of 90°. Observer JD.

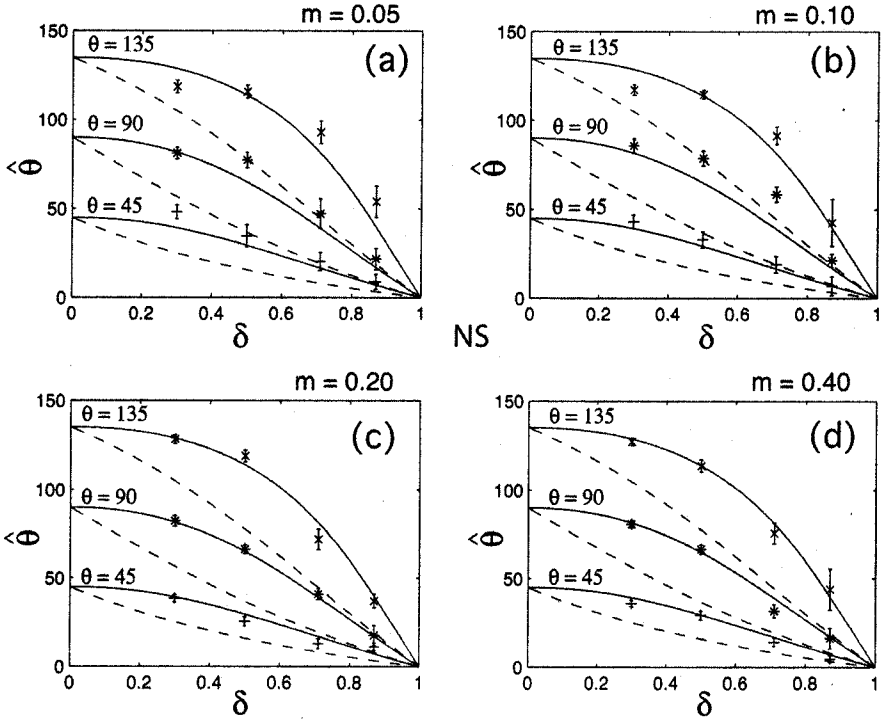


Figure 15.7. Results of experiment 1 for observer NS. See caption to Figure 15.6.

The data of experiment 1 are explained simply as the attenuation of the lower-contrast stimulus by a factor of $\delta^{\gamma}$ before binocular combination. This relationship is derived from the gain-control model. The following experiments investigate factors that determine the relative weights of the stimuli in the two eyes to enable estimation of other parameters of the gain-control model.

## 15.4 Experiment 2. Stimulus duration

### 15.4.1 High contrast energy vs. low contrast energy

The gain-control model of binocular combination described below has two properties that are relevant to experiment 1 and bear further investigation. As the contrast energy, $\mathcal{E}_L$ and $\mathcal{E}_R$, of input sinewave stimuli is reduced, the gain-control model asymptotically approaches simple linear summation. As the contrast energy $\mathcal{E}_{max}$ of the greater of two sinewave inputs is increased, the model's output becomes asymptotically independent of $\mathcal{E}_{max}$.

In experiment 1, the contrast energies $\mathcal{E}_{max}$ were quite high and, indeed, the shapes of the model predictions were virtually independent of the contrast of the higher-contrast sinewave grating. Experiment 2 was designed to investigate whether the gain-control

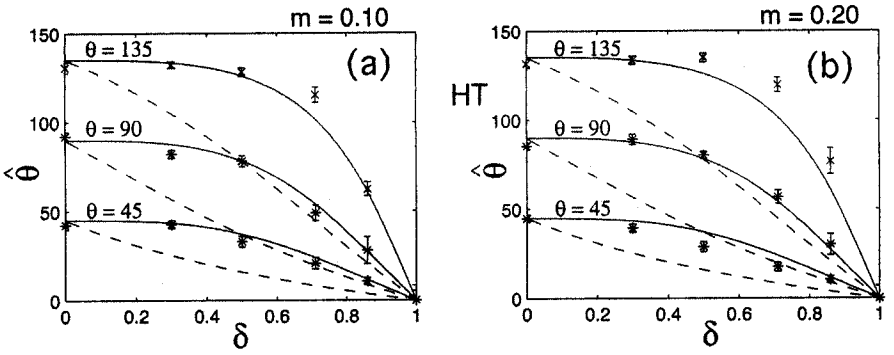


Figure 15.8. Results of experiment 1 for observer HT. See caption to Figure 15.6. The results for the control conditions $\delta = 0$, $\delta = 1$, are also shown here.

model remains valid when input gratings have low contrast energies, to investigate binocular combination over a range of contrast energies, and thereby to determine the time-constant of interocular gain control.

## 15.4.2 Stimuli

In experiment 1, the reference lines and the sinewave stimulus to be judged appeared simultaneously for 1000 ms. This simultaneity did not yield reliable data with very brief exposures. Figure 15.10 shows the slightly modified procedure used in experiment 2. Unlike experiment 1, the reference line was presented in advance of the input sinewave gratings. The reference line appeared 500 ms before the input sinewave grating was presented and remained on for 1500 ms. The duration of input sinewave gratings varied from 50 ms to 1000 ms. The stimuli used in experiment 2 are given by Eqs. (15.1) and (15.2) as in experiment 1 except that, where the stimulus duration $T$ (Eq. (15.3)) in experiment 1 was fixed at 1000 ms, in experiment 2, $T$ varied from 50 ms to 1000 ms.

Only one phase difference $\theta = 90°$ between the left- and right-eye sinewave gratings was used. Two contrasts of the higher-contrast grating were studied: 10% and 20%. The contrast ratio $\delta$ of the lower to the higher contrast sinewave grating took values of 0, 0.3, 0.5, 0.71, and 0.86. The following exposure durations were used: 50, 100, 200, 400, and 1000 ms. Each condition ($m$ contrast of higher-contrast grating, $\delta$ contrast ratio, $T$ exposure duration) was run in the four variations in Figure 15.4. All $2{\times}5{\times}5{\times}4 = 200$ conditions (10 000 trials) were run in a mixed-list design with interleaved up-down staircases. One experienced observer (HT) served as the observer.

## 15.4.3 Results

Figure 15.11 shows the results of experiment 2. Each panel shows a different combination of exposure duration and of contrast of the higher-contrast sine wave. In the control conditions, $\delta = 0$, the measured apparent phase difference was consistently very close to 90°, indicating that the observer was able to make reliable judgments of

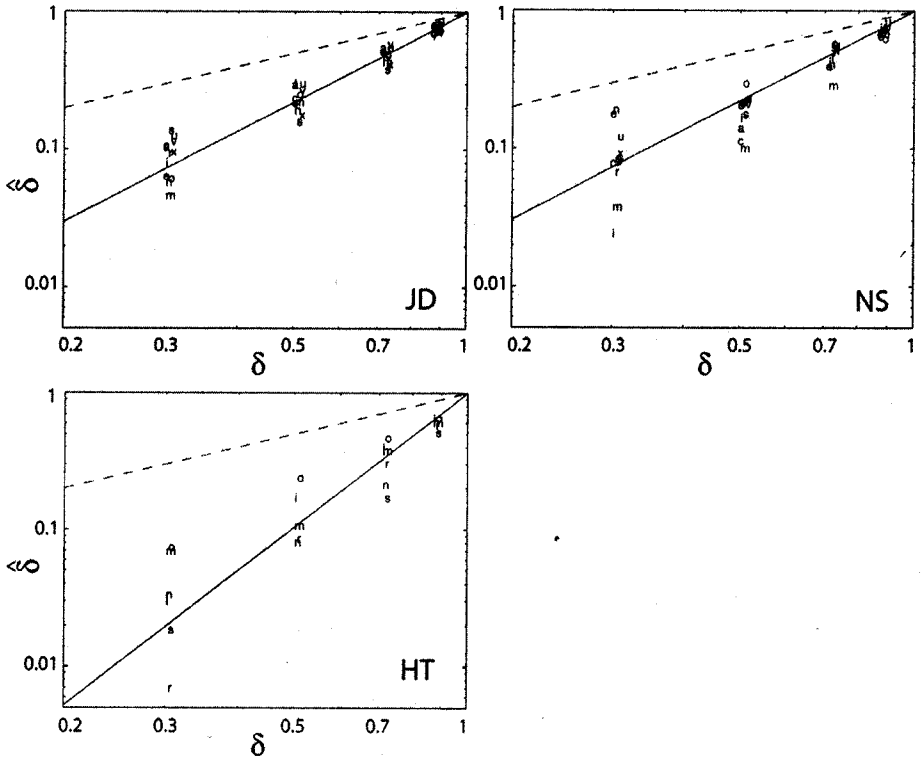


Figure 15.9. Experiment 1 analysis. How the interocular contrast ratio affects binocular combination: A log-log plot of the apparent interocular contrast ratio $\hat{\delta}$ as a function of the actual interocular contrast ratio $\delta$. The apparent interocular contrast ratios $\hat{\delta}$ are calculated from the perceived phase shifts $\hat{\theta}$ of Figures 15.6, 15.7, and 15.8. The dashed lines are predicted by algebraic (linear) summation of left- and right-eye stimuli. The gain-control model predicts that, within measurement error, data for all interocular phase differences and for all contrasts of the higher-contrast grating collapse onto a single straight line with a slope equal to $1+\gamma$, where $\gamma$ is the exponent of the rectifying power function in the gain-control path. For observers JD, NS, and HT, respectively, $\gamma$ = 1.18, 1.17, and 2.27. The data points are represented by letters: a, $m = 0.05$ and $\theta = 45°$; c, $m = 0.05$ and $\theta = 90°$; e, $m = 0.05$ and $\theta = 135°$; i, $m = 0.10$ and $\theta = 45°$; m, $m = 0.10$ and $\theta = 90°$; n, $m = 0.10$ and $\theta = 135°$; o, $m = 0.20$ and $\theta = 45°$; r, $m = 0.20$ and $\theta = 90°$; s, $m = 0.20$ and $\theta = 135°$; u, $m = 0.40$ and $\theta = 45°$; v, $m = 0.40$ and $\theta = 90°$; x, $m = 0.40$ and $\theta = 135°$. The increase in log variability as $\delta$ decreases merely indicates that the variabilities of phase judgments tend to remain constant, independent of $\delta$, and therefore for small $\delta$ log variability in $\hat{\delta}$ increases proportionally to $\log(1/\delta)$.

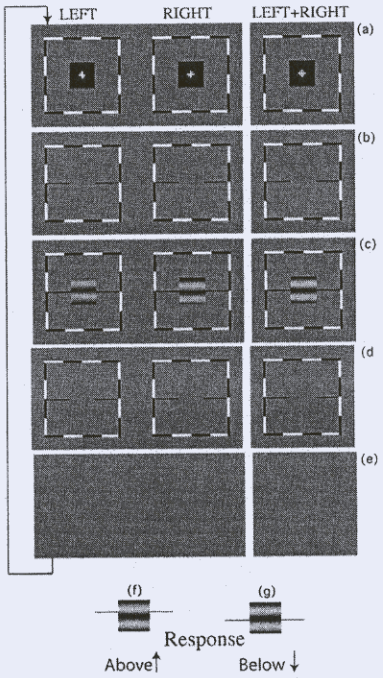


Figure 15.10. Procedure of experiment 2. How stimulus duration affects binocular combination. The procedure is similar to that of experiment 1 (see Figure 15.3). The differences are: (b) the reference lines appear 500 ms before the stimuli are presented; (c, d) the reference lines remain for 1500 ms; and the duration of the stimuli (c) varies from 50 ms to 1000 ms.

location. The dashed curves of Figure 15.11 are predictions of simple linear summation. The solid curves are the best fit of the gain-control model with one additional parameter, the time constant of interocular gain-control (563 ms).

For the short stimulus duration (50 ms) and lowest contrast (of the higher-contrast sinewave grating, 10%), the data are quite well described by linear summation of the inputs of the two eyes. However, as duration and contrast increased, the deviations from linear summation become greater. For the the highest contrast and duration, deviation from the linear model is extreme. Note also that in Figure 15.11, combinations with equal contrast energy produce similar data: e.g., $m = 0.1 \times T = 100$ and $m = 0.2 \times T = 50$, $m = 0.1 \times T = 200$ and $m = 0.2 \times T = 100$, and $m = 0.1 \times T = 400$ and $m = 0.2 \times T = 200$.

Figure 15.12 shows the results in a plot of the perceived phase shift $\hat{\theta}$ versus the stimulus duration $T$ for a fixed contrast ratio of 0.5 for two observers. The data are the same as in Figure 15.11 when $\delta = 0.5$. The dashed line indicates the prediction of the linear model. The solid curve is derived from the same gain-control model as in Figure 15.11.

Figure 15.13 shows the effective interocular contrast ratio $\hat{\delta}$ as a function of the

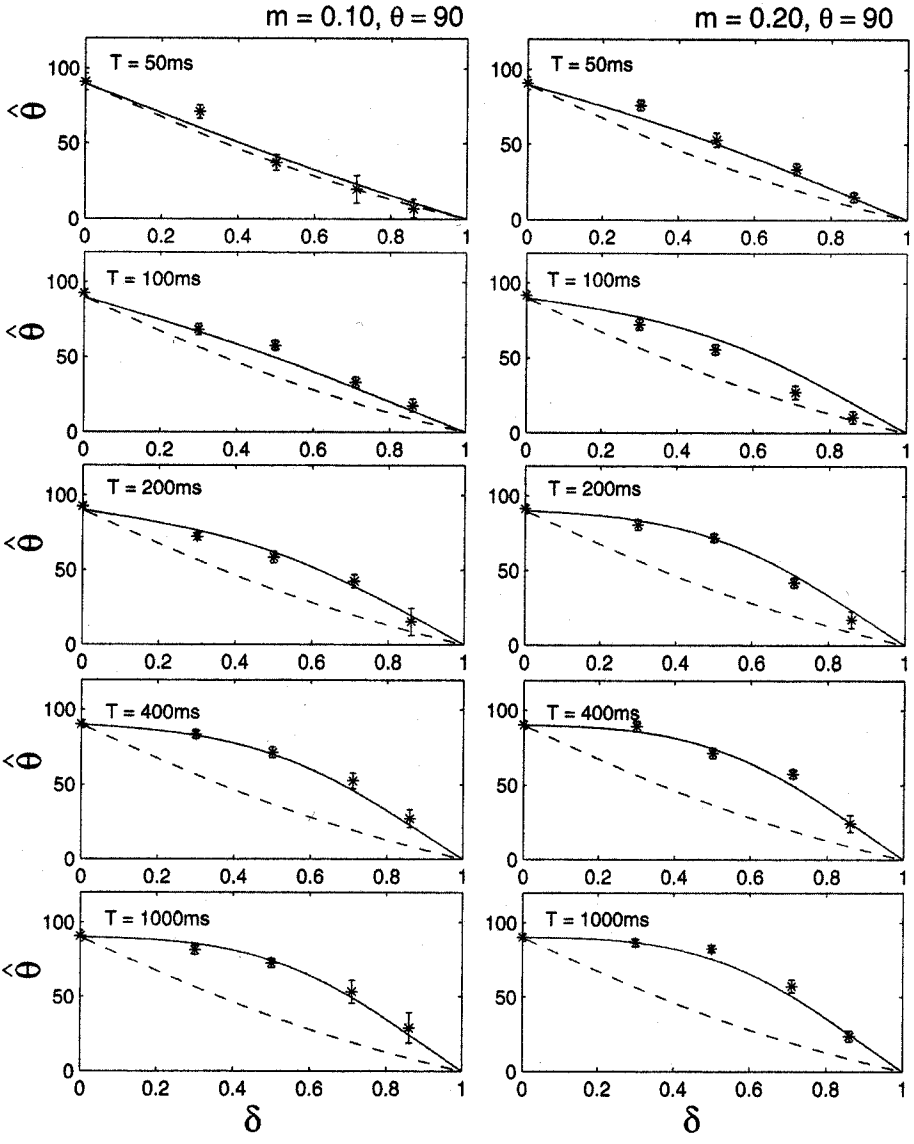


Figure 15.11. Results of experiment 2. How stimulus duration affects binocular combination. Perceived phase shift $\hat{\theta}$ as a function of interocular contrast ratio $\delta$ for stimulus durations from 50 ms to 1000 ms. Each row of panels shows a different duration $T$ of the stimulus gratings. For the left column of panels, the contrast $m$ of the higher-contrast grating is 0.10, for the right column, $m = 0.20$. The interocular grating phase difference $\theta$ was fixed at 90°. The dashed lines are the predictions based on algebraic (linear) summations of left- and right-eye stimuli; the solid lines are best fits of the gain-control model. Observer HT.

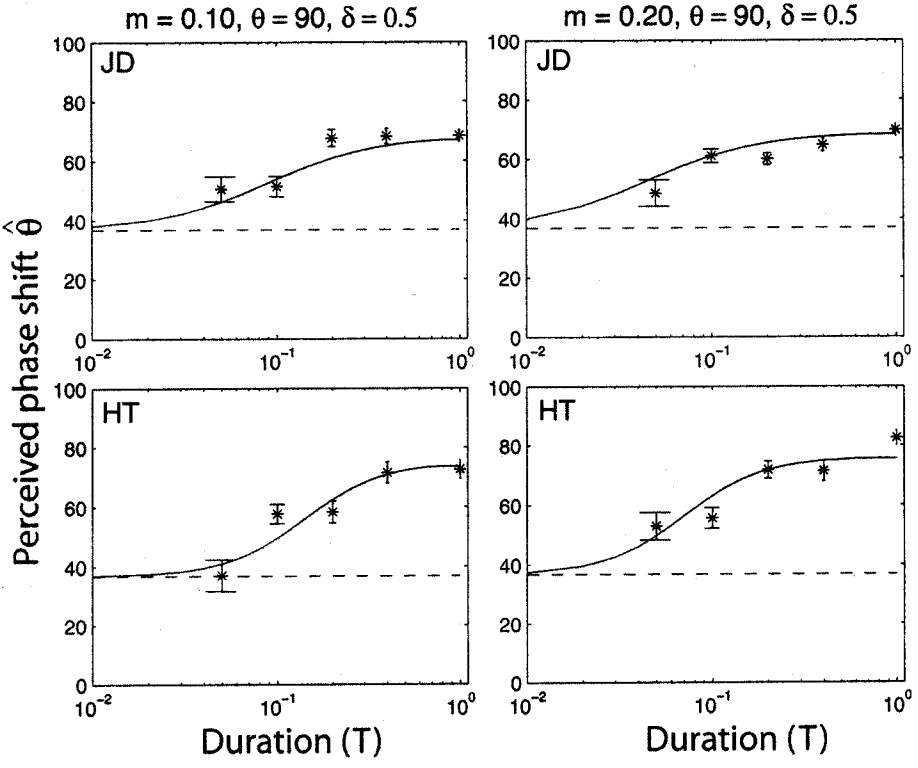


Figure 15.12. Summary of experiment 2. How stimulus duration affects binocular combination: Perceived phase shift $\hat{\theta}$ as a function of stimulus duration $T$ for a fixed interocular contrast ratio $\delta = 0.5$. The interocular grating phase difference $\theta$ is 90°; the contrast $m$ of the higher-contrast grating is 10% (left column) or 20% (right column). Top panels: Observer JD. Experimental data were obtained only for $\delta = 0.5$. Bottom panels: Observer HT. Data are taken from Figure 15.11 for $\delta = 0.5$. Dashed lines are predictions based on algebraic (linear) summations of the left- and right-eye stimuli; solid lines are best fits of the gain-control model.

actually presented contrast ratio $\delta$ in log-log coordinates. The solid curves are predictions from the best fitting gain-control model in Figure 15.11 transformed into this new coordinate system. All the data curves lie between the two asympototes. The upper asymptote line is $\hat{\delta} = \delta$, the prediction from linear summation. The lower asymptote is $\hat{\delta} = \delta^{1+\gamma}$, the prediction from the same gain-control model with infinite contrast energy or, equivalently, $k = 0$. As the stimulus duration increased from 50 ms to 1000 ms and the contrast of higher-contrast sinewave grating increased from 10% to 20%, the stimulus contrast energy increased from the low values that approached the upper asymptote to high values of contrast energy that approached the lower asymptote. For all values of contrast energy, the data are confined to lie laminarly between these two asymptotes.

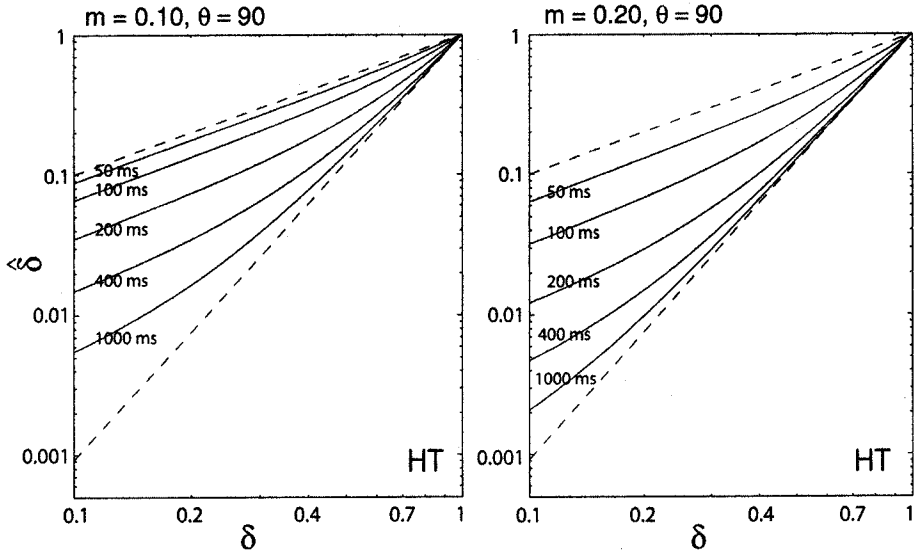


Figure 15.13. Experiment 2 analysis. How stimulus duration affects binocular combination. A log-log plot of the apparent interocular contrast ratio $\hat{\delta}$ as a function of the actual interocular contrast ratio $\delta$ for two contrasts of the higher-contrast stimulus and five different stimulus durations. The top dashed lines are derived from algebraic (linear) summations of the left- and right-eye images, i.e., $\hat{\delta} = \delta$. The solid lines are replotted from Figure 15.11 and represent the best fits of the gain-control model with the following parameters: a rectifying, power-law exponent $\gamma = 2.04$, a simple exponental temporal filter in the gain control path with time constant $\tau = 0.563$ s, and a gain-control threshold energy $k = 2.18 \times 10^{-4}$ s, e.g. 50 ms $\times$ contrast 0.436%. The bottom dashed lines are predictions of the gain-control model with a stimulus of infinite duration (or energy), or equivalently, when $k = 0$.

## 15.5 Experiment 3. Masking by spatial-frequency noise

### 15.5.1 Total contrast energy versus signal contrast energy

The gain-control model described by Eq. (15.9) predicts that the eye presented with a higher-contrast contrast energy stimulus will dominate binocular combination. In experiments 1 and 2, all contrast energies were perfectly correlated with the signal being judged. In experiments 3–6, one eye received an irrelevant stimulus, a "masking" stimulus, in addition to the stimulus being judged in order to determine the effect of the "mask" on ocular dominance. In all these experiments, the eyes were presented, as previously, with the 0.68° horizontal sinewave gratings in which the location of the cyclopean dark stripe was to be judged. The gratings were identical in contrast ($\delta = 1$) and differed only by a phase shift of $\theta = 90°$.

In experiment 3, the signal to one of the eyes also had added bandpass noise. If gain control was produced only by signal energy, the perceived phase shift would be

0° for all levels of noise as $\delta = 1$. If the gain control were caused by the total contrast energy, the eye simultaneously presented with the added noise would dominate in binocular combination because the eye receiving the added noise would have more contrast energy.

### 15.5.2 Stimuli

In experiment 3, the two sinewave gratings being judged were both of contrast 0.1 and differed in phase by 90°. A bandpass noise, produced by filtering a two-dimensional binary random noise $R(x, y)$ with a 2D isotropic bandpass filter (Rainville and Kingdom, 2002), was superimposed on the sinewave grating presented to one eye. In the spatial frequency domain, the isotropic bandpass filters are defined as

$$Q(u, v, f_{s,N}) = \exp\left(-\frac{1}{2}\left(\frac{\ln(f/f_{s,N})}{\ln(\sigma)}\right)^2\right), \tag{15.5}$$

where $u$ and $v$ are the dimensions of a two-dimensional Cartesian spatial-frequency coordinate system, $f$ is defined as $\sqrt{u^2 + v^2}$, $f_{s,N}$ is the center spatial-frequency, and $\sigma$ determines the bandwidth of the filter. Six bandpass filters having different values of center spatial-frequency were used in the experiment. Their center spatial-frequencies, $f_{s,N}$, were separated by an octave, and are {0.34, 0.68, 1.36, 2.72, 5.44, 10.88 cpd}. The half-amplitude bandwidth of the various noise masks was a factor of 2.4 (1.26 octaves). A spatial bandpass filtered noise $\widetilde{\mathcal{M}}(x, y, f_{s,N})$ was obtained via a reverse Fourier transform: $\widetilde{\mathcal{M}}(x, y, f_{s,N}) = Re(\mathcal{F}^{-1}\{Q(u, v, f_{s,N})\mathcal{F}(R(x, y))\})$. Normalizing a bandpass noise $\widetilde{\mathcal{M}}(x, y, f_{s,N})$ by its RMS contrast yielded a "standard" noise $\mathcal{M}(x, y, f_{s,N})$ with RMS contrast 1.0, i.e.,

$$\mathcal{M}(x, y, f_{s,N}) = \frac{\widetilde{\mathcal{M}}(x, y, f_{s,N})}{\mathrm{RMS}(\widetilde{\mathcal{M}}(x, y, f_{s,N}))}. \tag{15.6}$$

The stimuli in experiment 3 are given by Eqs. (15.1) and (15.2), where the mask $\mathcal{M}$ is given by Eq. (15.6), $m_L = m_R$, $\theta_L - \theta_R = \pm 90°$, and one of $n_L$ and $n_R$ (the RMS contrast of the bandpass masking noise in one eye) was set to be zero. The values of $m$ and $n$ were constrained so that less than 5% of pixels fell outside the range of contrast values that can be produced on the display screen.

Sample stimuli are shown in the top of Figure 15.14. Figure 15.14 (L) illustrates a sinewave grating presented (for example) to the left eye and Figure 15.14 (R) illustrates a similar grating presented to the right eye phase-shifted 90° and with added bandpass noise. A sample of a signal plus noise in each frequency band is shown in the inset on each plot.

The procedure for experiment 3 was the same as that for experiment 1. For each combination of center spatial-frequencies, $f_{s,N}$, and noise-signal ratios $N/S = n/m$ there are four variations: dark stripe up/down × mask L/R. All 6×4×4 = 96 conditions were run in a mixed-list design with interleaved up-down staircases. Two experienced observers served in the experiment.

### 15.5.3 Results

Figure 15.14 shows the results of experiment 3. The abscissa indicates the root-mean-square (RMS) contrast ratio of the noise to the signal (N/S), and the ordinate indicates perceived phase shift, $\hat{\theta}$. When $\hat{\theta} = 0$, both eyes have equal contributions to binocular combination. When $\hat{\theta} > 0$, it indicates that the eye with the added noise mask dominated the binocular combination. All of the data show that the eye which receives the added noise dominates binocular combination. The greater the noise energy, the greater the domination. Remarkably, the greatest domination occurred at a frequency (2.72 cpd) that is 4× the frequency being judged. At equal contrast ($N/S = 1$) there was almost complete domination, a phase shift of 80° out of a possible 90°. Contrary to a Bayesian point of view which would suggest that a noisy stimulus should have less influence in binocular combination than a noiseless one, the noisy stimulus dominates up to and beyond the point where it has obliterated the stimulus being judged so that location judgments are no longer possible (e.g. Figure 15.14 b and c).

Figure 15.15 shows the data of a second observer. The spatial frequency modulation transfer function derived from these data is shown in the model section (below).

## 15.6 Experiment 4. Masking sinewave gratings of different spatial frequencies

### 15.6.1 Masking sinewave gratings in experiments 4, 5, and 6

In experiments 4, 5, and 6, as in experiment 3, the left- and right-eye sinewave gratings are of the same contrast and differ only in phase, $\theta = 90°$. A masking sinewave grating, given by

$$\mathcal{M}(x, y, f_{s,mask}, f_{t,mask}, \beta) = \sin(2\pi f_{s,mask}(x\cos\beta + y\sin\beta) \pm 2\pi f_{t,mask}t + \theta_{mask}), \tag{15.7}$$

was superimposed on one eye's sinewave grating.

### 15.6.2 Stimuli

In experiment 4, the stimuli are given by Eqs. (15.1) and (15.2) where $\mathcal{M}$ is given by Eq. (15.7), $m_L = m_R = 10\%$, $\theta_L - \theta_R = \pm 90°$, and one of $n_L$ and $n_R$ was set to be zero.

The mask was a static vertical sinewave grating; its spatial frequency $f_{s,mask}$ was chosen from among $\{0.34, 0.68, 1.36, 2.72, 5.44, 10.88\}$ cpd, $\beta = 90°$ (the angle between horizontal grating being judged and the the masking grating), and $f_{t,mask} = 0$. For each combination of the spatial frequency $f_{s,mask}$ and mask-to-signal contrast ratio $M/S$, there were four variations: dark stripe up/down × mask L/R. The procedure for experiment 4 was the same as that for experiment 1. All $6 \times 5 \times 4 = 120$ conditions were run in a mixed-list design with interleaved up-down staircases. Two experienced observers served in the experiment.

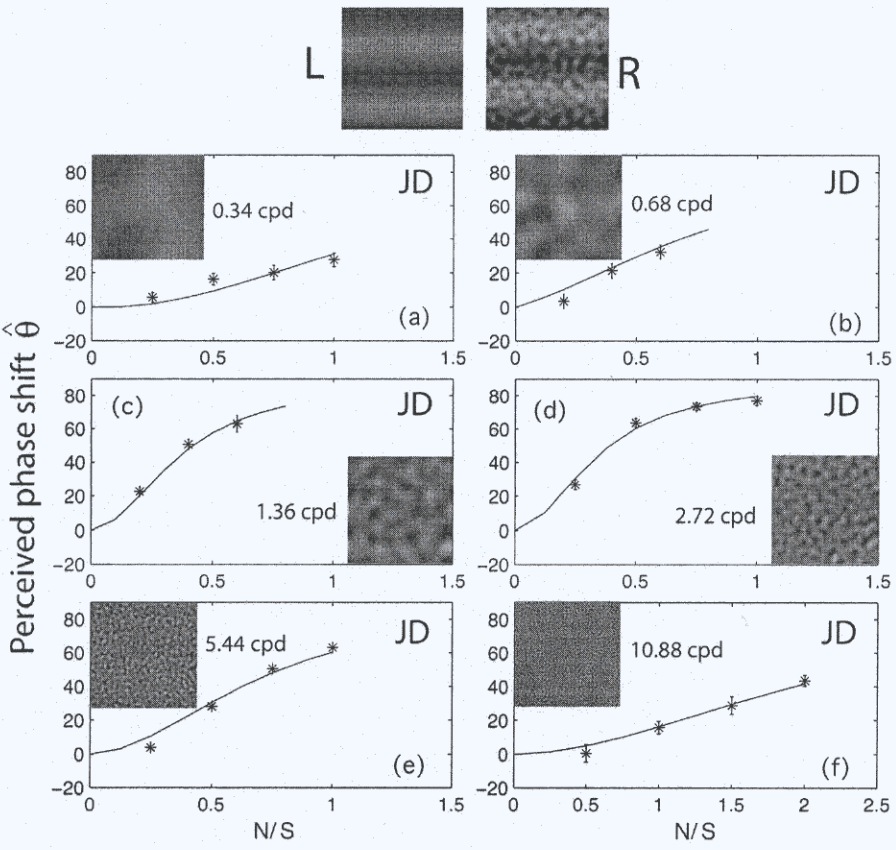


Figure 15.14. Experiment 3. How the spatial frequency and contrast of added 2D noise in one eye increase its binocular dominance. (L, R) A sample binocular stimulus to the left and right eyes. Panels (a)–(f) show the perceived phase shift $\hat{\theta}$ as a function of the ratio of RMS noise to RMS signal, $N/S$. The horizontal grating contrast (signal) $S$ was 0.1 and was equal in both eyes (interocular contrast ratio $\delta = 1$). The interocular grating phase difference $\theta$ was 90°. The central spatial frequency (in cycles per degree of visual angle, cpd) of the noise is indicated in each panel. The half-amplitude bandwidth of the various masking noise stimuli was a factor of 2.4 (1.26 octaves). The signal has a spatial frequency of 0.68 cpd. Data collection was continued until N/S was either too great to permit judgments of phase (e.g. panels (b), (c)) or until the limits of the apparatus were reached (other panels). The solid lines are the best fits derived from the gain-control model. Adding noise to one eye at 2.72 cpd with an RMS amplitude equal to that of the binocular signal being judged gave the masked eye virtually complete binocular domination, i.e. produced a phase shift of 80° of a maximum possible 90° (a 90° phase shift implies zero weight for the signal in the unmasked eye). Observer JD.

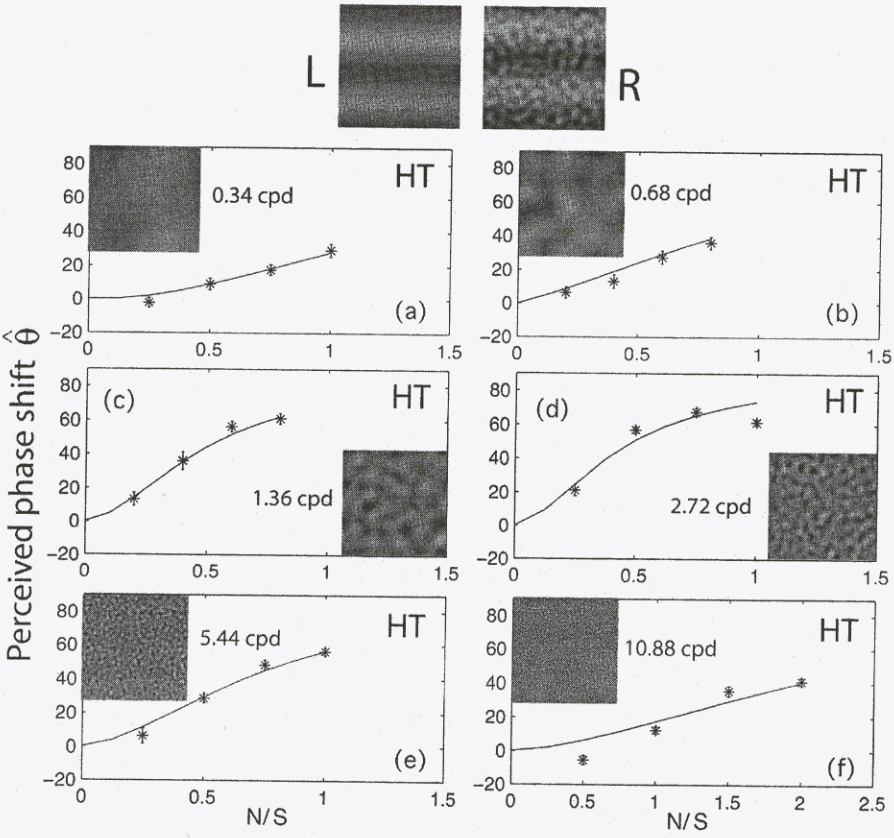


Figure 15.15. Experiment 3. How the spatial frequency and contrast of added 2D noise in one eye increases its binocular dominance. Observer HT. See caption to Figure 15.14.

### 15.6.3 Results

Figure 15.16 shows the results of experiment 4. The abscissa indicates the contrast ratio $M/S$ of mask to signal, and the ordinate indicates the perceived phase shift, $\hat{\theta}$. As in experiment 3, the data show that the eye receiving the grating mask dominates the summation. As mask contrast increased, domination increased. The data for sinewave masking as a function of spatial frequency were quite similar to those obtained in experiment 3 for band-limited noise masking as a function of spatial frequency. Figure 15.17 shows the results of a second observer. The spatial frequency modulation transfer function will be considered in the model section.

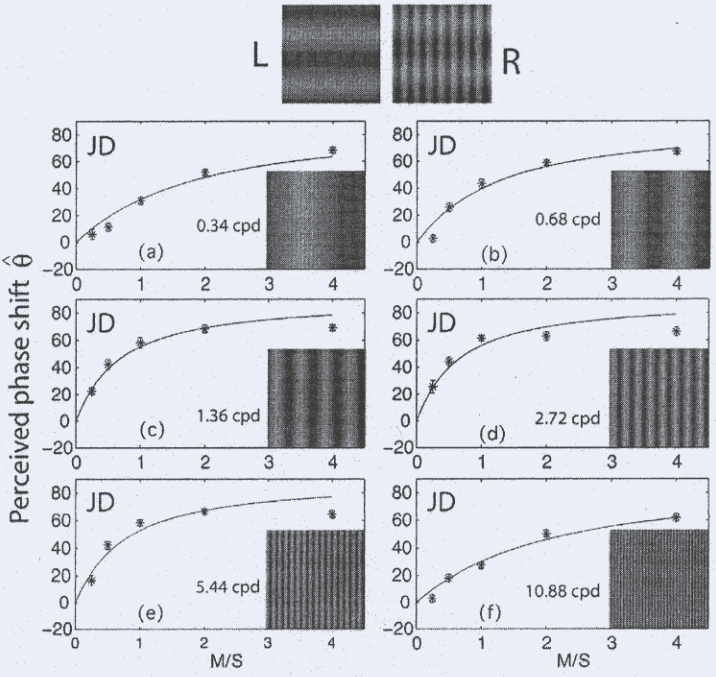


Figure 15.16. Results of experiment 4: How masking sinewave gratings of different spatial frequencies in one eye increase its dominance in binocular combination. (L, R) A sample binocular stimulus to the left and right eyes. Panels (a)–(f) show the perceived phase shift $\hat{\theta}$ as a function of the ratio $M/S$ of the amplitude $M$ of a vertical sinewave grating masking stimulus in one eye to the amplitude $S$ of the binocular horizontal sinewave signal whose phase was being judged. The spatial frequency (in cycles per degree of visual angle, cpd) of the vertical masking grating was indicated in each panel. The horizontal signal grating contrast $S$ was 0.1 and equal in both eyes (interocular contrast ratio $\delta = 1$). The interocular grating phase difference $\theta$ was 90°. The horizontal signal grating is 0.68 cpd. Data collection was continued until $M/S$ was at the limits of the apparatus. The solid lines are the best fits derived from the gain-control model. A masking-to-signal ratio M/S $\geq 2$ gave the masked eye overwhelming dominance in binocular combination. Observer JD.

## 15.7 Experiment 5. Temporal frequency masking

### 15.7.1 Stimuli

The procedure for experiment 5 was basically the same as that for experiment 4. The stimuli were the same as those in experiment 4, given by Eqs. (15.1) and (15.2) except that the added vertical mask was a drifting rather than a stationary sinewave grating. Mask parameters were $f_{s,mask} = 0.68$ cpd, the same spatial frequency as the signal, and $\beta = 90°$ (mask to signal angle, Eq. (15.7)).

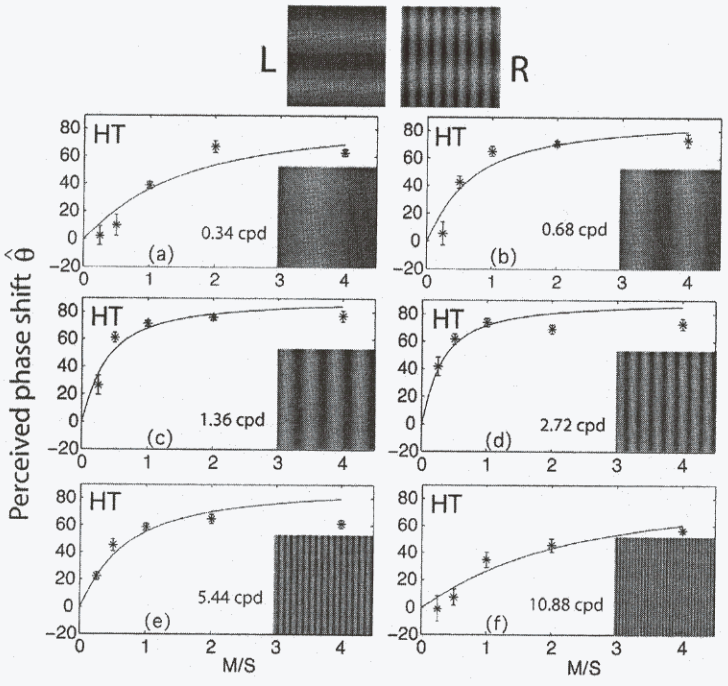


Figure 15.17. Results of experiment 4. How masking sinewave gratings of different spatial frequencies in one eye increase its dominance in binocular combination. Observer HT. See caption of Figure 15.16.

The independent variables were mask contrast, mask temporal frequency $f_{t,mask}$, four variations (dark stripe up/down × mask L/R), and mask movement direction (left, right). All $5 \times 5 \times 4 \times 2 = 200$ conditions were run in a mixed-list design with interleaved up-down staircases (5 000 trials). Two experienced observers served in the experiment.

## 15.7.2 Results

Figure 15.18 shows the results of experiment 5. The abscissa indicates the contrast ratio of mask to signal (M/S), and the ordinate indicates the perceived phase shift, $\hat{\theta}$. Again, the data show that the eye receiving – in this case – a drifting masking grating dominated the binocular combination. As mask contrast increased, domination increases for all temporal frequencies. In Figure 15.18f, the data from 0 Hz and 30 Hz are plotted together to illustrate that these two masking functions differ mainly by a horizontal translation, i.e. there was proportionally less masking at 30 Hz than for a stationary grating – or for that matter any lower temporal frequency. This low-pass characteristic of the temporal frequency modulation transfer function will be further considered below in the model section. Figure 15.19 shows the data of a second observer.

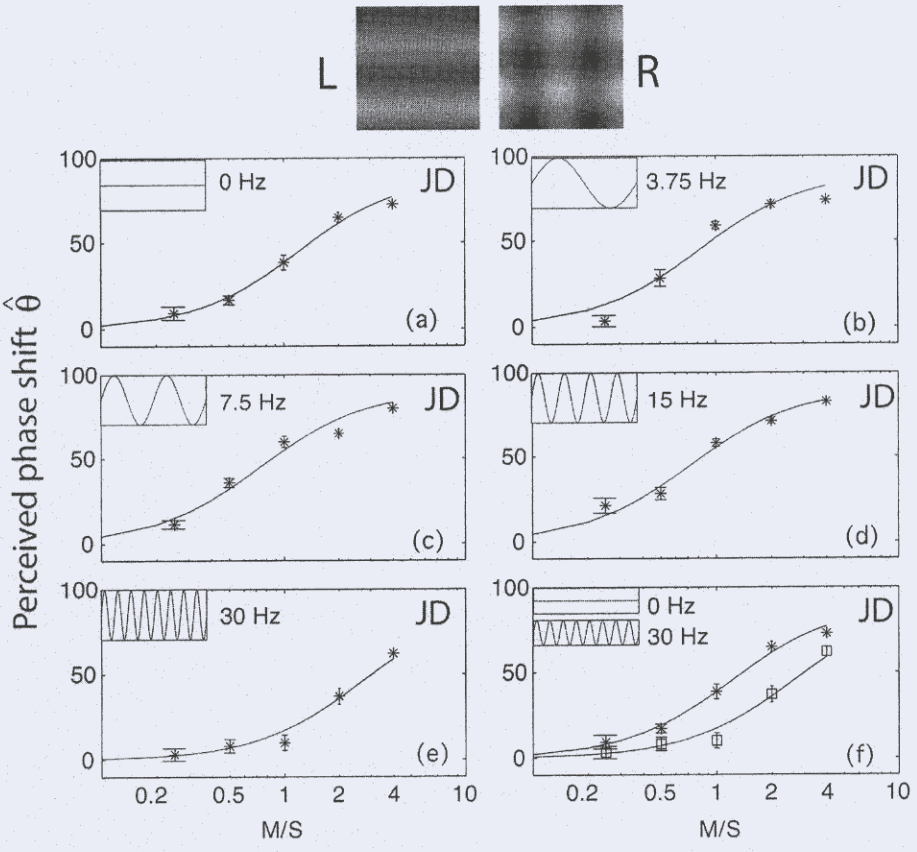


Figure 15.18. Results of experiment 5. How the temporal frequency and contrast of a dynamic masking grating in one eye increase its binocular dominance. (L, R) A sample left- and right-eye frame from a dynamic binocular stimulus. Panels (a)–(f) show the perceived phase shift $\hat{\theta}$ as a function of the ratio $M/S$ of the amplitude $M$ of a drifting vertical sinwave grating masking stimulus in one eye to the amplitude $S$ of the binocular horizontal sinewave signal whose phase is being judged. The horizontal signal and vertical masking grating both have a spatial frequency of 0.68 cpd. The horizontal signal grating contrast $S$ is 0.1 and equal in both eyes (interocular contrast ratio $\delta = 1$). The interocular grating phase difference $\theta$ is 90°. The vertical masking grating translates horizontally (randomly left or right from trial to trail) to produce temporal frequencies of 0–30 Hz as indicated in panels (a)–(f). For comparison, panel (f) shows the data for both 0 Hz masking (from panel a) and 30 Hz. Data collection is continued until $M/S$ is at the limits of the apparatus. The solid lines are the best fits derived from the gain-control model. At all temporal frequencies 0–30 Hz, a masking-to-signal amplitude ratio of 4 gives the masked eye overwhelming dominance in binocular combination. Observer JD.

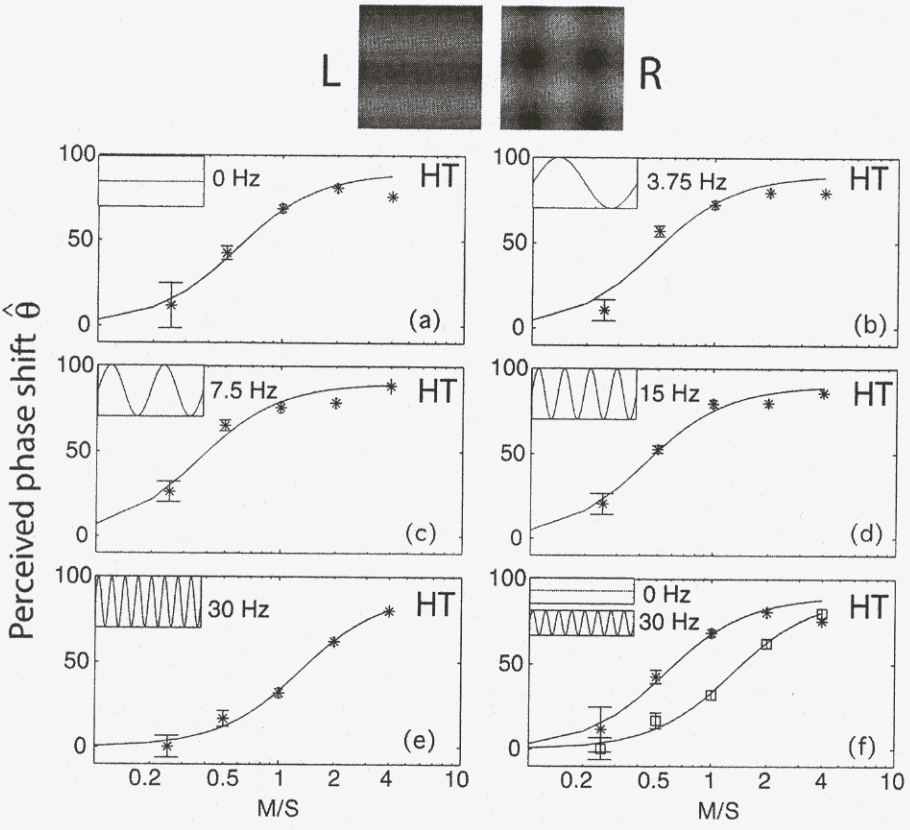


Figure 15.19. Results of experiment 5. How the temporal frequency and contrast of a dynamic masking grating in one eye increase its binocular dominance. Observer HT. See caption of Figure 15.18.

## 15.8 Experiment 6. Orientation masking

### 15.8.1 Stimuli

The procedure for experiment 6 was similar to that for experiment 4. The stimuli were the same as those in experiment 4, given by Eqs. (15.1) and (15.2), except that the orientation of the mask grating varied from trial to trial instead of being fixed at the vertical position. The parameters for the mask grating are described in Eq. (15.7): spatial frequency $f_{s,mask} = 5.44$ cpd (three octaves higher than that of the signal), temporal frequency $f_{t,mask} = 0$ (a static sinewave grating). The independent variables were mask contrast (5 levels) and mask orientation (9 levels). All $9 \times 5 \times 4 = 180$ conditions were run in a mixed-list design with interleaved up-down staircases. Two experienced observers served in the experiment.

### 15.8.2 Results

Figure 15.20 shows the results of Experiment 6. The abscissa indicates the contrast ratio of mask to signal ($M/S$) and the ordinate indicates the perceived phase shift, $\hat{\theta}$. Again, the data show that the eye receiving – in this case – an oriented, static masking grating dominates binocular combination. All orientations are effective in producing domination, but vertical and horizontal gratings seem to be somewhat better than diagonally oriented gratings. As mask contrast increases, domination increases for all orientations. That orientation angle affects masking indicates that the "receptive field" of the masking channels cannot be exclusively circularly symmetric which, in turn, implies that at least some portion of the gain control has a cortical origin. The orientation tuning function will be derived and discussed in the model section. Figure 15.21 shows the results of a second observer.

## 15.9 Model

There have been many experimental investigations and numerous theories proposed to describe binocular combination. A pervasive problem with these efforts has been that they typically operate on a principle that is less than a point-by-point binocular combination of images. Typically, the theories abstract a parameter from each eye's image (e.g., the maximum stimulus contrast or brightness, a contrast detection threshold, a signal-to-noise ratio, or the visual direction of a significant point) and combine the parameter values from each eye to predict the parameter value in the cyclopean image.

Previously (Ding and Sperling, 2006), we offered a gain-control theory that in principle could derive a cyclopean image from a point-by-point comparison of the monocular images, and which derived the desired cyclopean parameters from the cyclopean image itself (rather than simply from a combination of the monocular parameters). At present we have derived the parameters of the gain-control theory for just a single visual channel sensitive to horizontal sine waves around 0.68 cpd. It is not clear how these parameters will generalize to other channels nor how channels will combine. Nevertheless, this is a physiologically plausible approach to binocular processes in early vision. Here we represent the gain-control model, derive the model parameters from the experimental data, and show how the model can efficiently account for not less than 97% of the variance in the experimental data for all observers and experiments. We then extend the model's predictions, which here have been concerned entirely with the phase of binocularly combined gratings, to amplitude as well.

### 15.9.1 Linear summation

Suppose that binocular combination were a linear combination of the left- and right-eye images, i.e., $\hat{I}(x) = I_{\text{L}}(x) + I_{\text{R}}(x)$, where $I_{\text{L}}(x)$ and $I_{\text{R}}(x)$ are defined by Eqs. (15.1) and (15.2). The perceived phase shift $\hat{\theta}$ of $\hat{I}(x)$ (defined by Eq. (15.4)) is then given by

$$\hat{\theta} = 2\tan^{-1}\left(\frac{1-\delta}{1+\delta}\tan\left(\frac{\theta}{2}\right)\right). \tag{15.8}$$

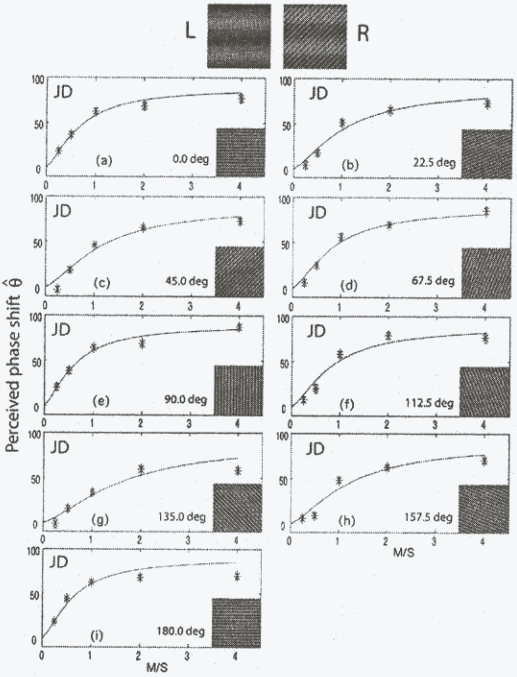


Figure 15.20. Results of experiment 6. How the orientation and contrast of a masking grating in one eye increase its binocular dominance. (L, R) A sample binocular stimulus to the left and right eyes. Panels (a)–(i) show the perceived phase shift $\hat{\theta}$ as a function of the ratio $M/S$ of the amplitude $M$ of a sinewave grating masking stimulus (in one eye) to the amplitude $S$ of the binocular horizontal sinewave signal whose phase was being judged. The signal grating contrast $S$ was 0.1 and was equal in both eyes (interocular contrast ratio $\delta = 1$). The interocular grating phase difference $\theta$ was 90°. The spatial frequency of the masking grating was 5.44 cpd, 3 octaves higher than that of the 0.68 cpd horizontal signal grating whose phase was being judged. The angle of the monocular masking grating (relative to the binocular signal grating) is indicated in each panel (a)–(i). Data collection was continued until $M/S$ is at the limits of the apparatus. The solid lines are the best fits derived from the gain-control model. At all orientations, masking stimuli that have contrasts 2 times greater than the binocular stimulus being judged gave the masked eye almost total ocular dominance. Observer JD.

Equation 15.8 defines the dashed lines (linear predictions) in Figures 15.6, 15.7, 15.8, 15.11 and elsewhere. The linear summation model's prediction connects with the data only at the end points – the nominal control conditions – in which $\delta = 0$ and $\delta = 1$ (which do not require measurement). The linear prediction does not match any of the actual data except those obtained with near-threshold stimuli.

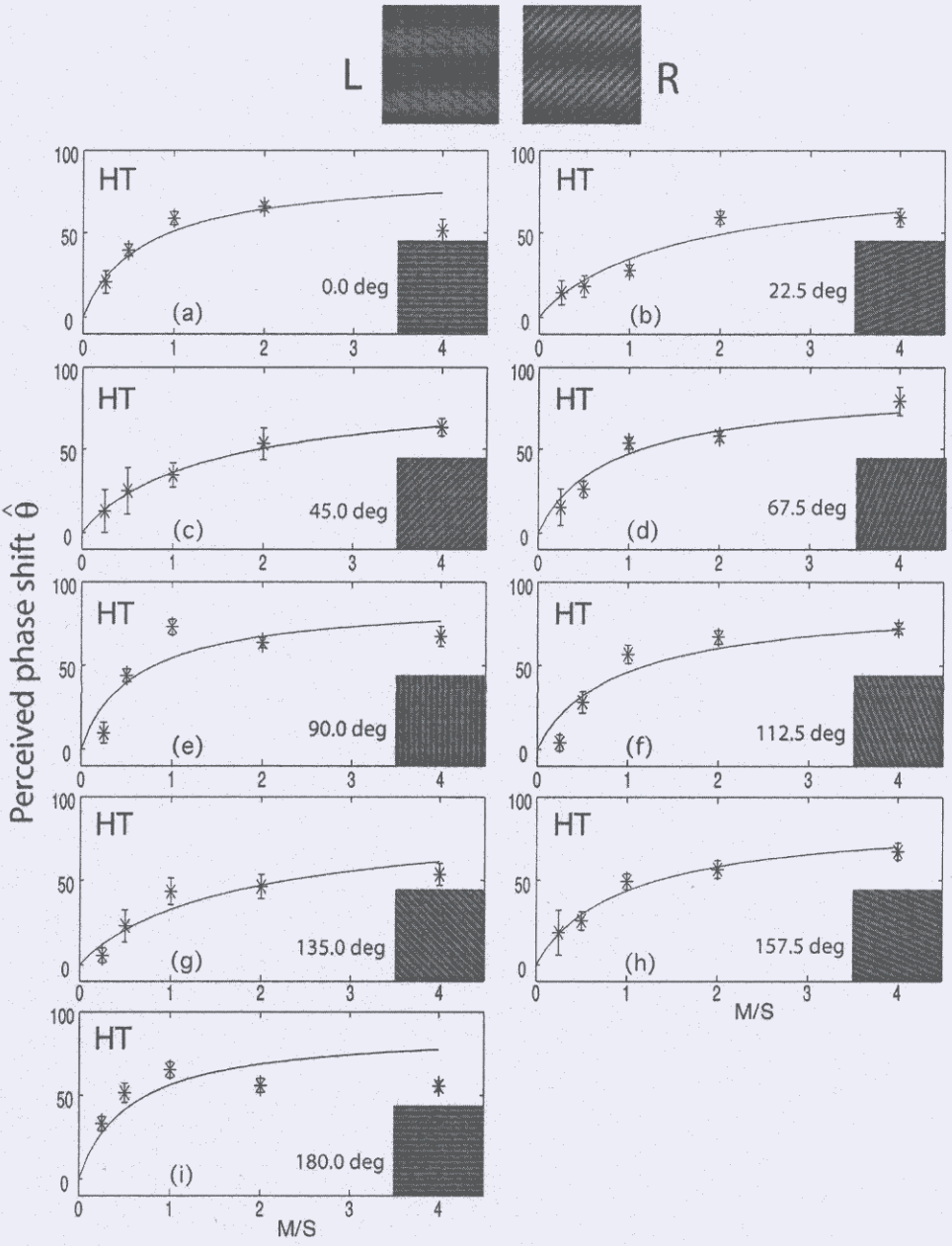


Figure 15.21. Results of experiment 6. How the orientation and contrast of a masking grating in one eye increase its binocular dominance. Observer HT. See caption of Figure 15.20.

### 15.9.2 Gain-control model

The problem with the linear model is that the eye with the higher-contrast stimulus has a greater advantage (or equivalently, the eye with the lower-contrast stimulus has a greater disadvantage, or both) than is predicted by algebraic addition of the stimuli. How does this come about? How does the brain attenuate the weaker stimulus prior to binocular combination? The gain-control model of Figure 15.22 (Ding and Sperling, 2006) is our attempt to answer this question. In every neighborhood, each eye exerts gain control on the other eye in proportion to the strength of its own input. The eye receiving the lower-contrast stimulus not only has a weaker stimulus but also receives the stronger gain-control signal from the other eye which has the higher-contrast stimulus.

Normalizing the gain control itself solves a lot of problems. We propose that an eye, say the left eye, not only gain-controls the right eye's output but also the right eye's attempt to control the left eye's output. These dual gain control mechanisms give the model the extraordinary property that, for equal stimuli to the two eyes which are sufficiently above threshold, closing one eye does not change the output of the model, emulating a profound property of natural vision. As shown in Figure 15.22a, the output $\hat{I}$ of the model is

$$\hat{I} = \frac{1+\mathcal{E}_L}{1+\mathcal{E}_L+\mathcal{E}_R} I_L + \frac{1+\mathcal{E}_R}{1+\mathcal{E}_L+\mathcal{E}_R} I_R, \tag{15.9}$$

where $\mathcal{E}_L$ and $\mathcal{E}_R$ are the total contrast energies of the images presented to the two eyes respectively. When $\mathcal{E}_L \gg 1$ and $\mathcal{E}_R \gg 1$, Eq. (15.9) becomes

$$\hat{I} \approx \frac{\mathcal{E}_L}{\mathcal{E}_L+\mathcal{E}_R} I_L + \frac{\mathcal{E}_R}{\mathcal{E}_L+\mathcal{E}_R} I_R, \tag{15.10}$$

from which the one-eye-equals-two-eyes property is immediately apparent.

### 15.9.3 Total visually weighted Contrast Energy (TCE)

The results from experiment 3 show that the gain-control mechanism depends not only on the stimulus contrast in the channel being judged, but on a wide range of channels, the most effective ones being 4× higher in spatial frequency. The model assumes that a quantity, the "Total visually weighted Contrast Energy" (TCE) of a stimulus, is used for the gain-control mechanism. Experiment 2 showed that gain control depended on exposure duration or, more precisely, on total contrast energy. Spatial frequency (experiments 3,4), temporal frequency (experiment 5), and orientation of a masking stimulus (experiment 6) all affect binocular combination. We assume therefore that the gain-controlling contrast energy is a weighted sum over all spatial frequency channels. We have not investigated how the TCE depends on the spatial arrangement of the contributing channels.

Figure 15.22b illustrates the computation of Total visually-weighted Contrast Energy (TCE) for the left eye. Let $I_L$ be the input image to the left eye and $I_{L,i}$ be the output of the temporal filter $h_{L,i}(t)$ within the $i$th spatial-frequency-and-orientation

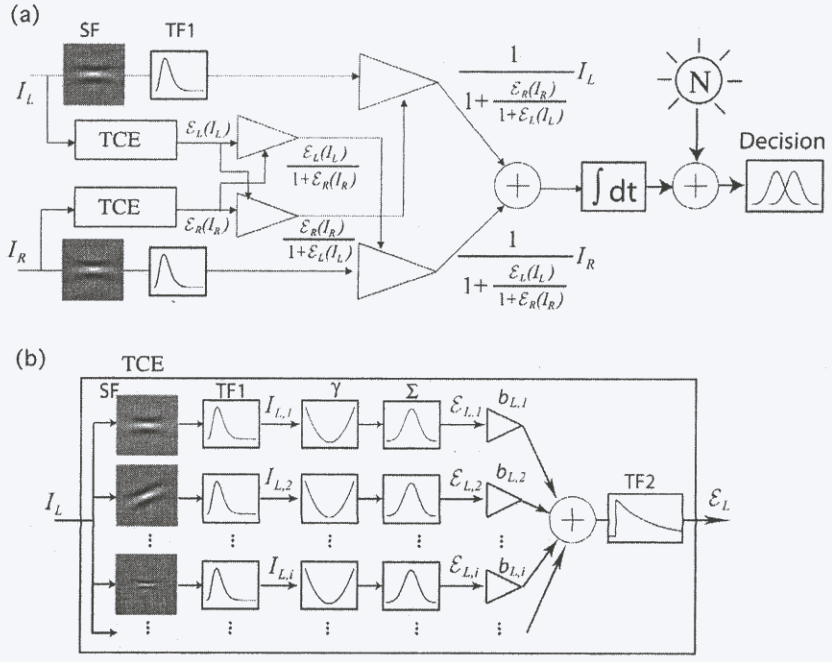


Figure 15.22. Gain-control model for binocular combination within a single binocular channel. (a) Block diagram of the model. The luminance stimuli to each eye, $I_L$ and $I_R$, are considered as being split into two channels: a stimulus analysis channel which, in this case, is selective for 0.68 cpd horizontal sine waves, and a gain-control channel that computes the Total visually weighted Contrast Energy, TCE. The stimulus analysis channels from the two eyes add their outputs to produce the cyclopean image. Triangles indicate shunting gain-control "amplifiers" in which the input is divided by a gain-control signal to produce the output. Prior to the addition of the signal channels, the TCE in each eye exerts shunting gain control on the signal of the opposing eye (top and bottom triangles). Additionally, the TCE in each eye also exerts gain control on the other eye's gain-control signal (middle triangles). This model of binocular combination has the remarkable property that when only one eye has a stimulus and the other eye has a blank, the output is asympotically the same as when both eyes have the same stimulus. To extend the model of binocular combination to apply to the present psychophysical experiments, three additional components are required. An integrator that integrates the total output of the model for the duration of a trial; random noise that is added to the integrated output; and a decision component that makes an optimal response based on the input it receives. (b) The computation of Total visually weighted Contrast Energy (TCE). The visual stimulus is processed separately in spatial-frequency-and-orientation channels, i.e. within each spatial frequency band, there are separate channels for each orientation. Channels overlap in spatial frequency, in orientation, and in space. In each gain-control channel, the signal is first temporally filtered by a lowpass filter (TF1) whose properties are defined by experiment 5, power-law rectified with exponent ($\gamma$), passed through a summing filter that sums over a wide spatial area ($\sum$), and assigned a weight $b_{L,i}$ that is specific for the particular pair of channels involved (signal, gain-control). TCE is the weighted sum of many such channels, only three of which are illustrated, and averaged over a relatively long period of time by a simple one stage RC filter TF2 whose time-constant is determined by experiment 2.

channel $g_{\mathrm{L},i}(x,y)$. Then

$$I_{\mathrm{L},i}(x,y,t) = \int g_{\mathrm{L},i}(x'-x,y'-y)h_{\mathrm{L},i}(t'-t)I_{\mathrm{L}}(x',y',t')\mathrm{d}x'\mathrm{d}y'\mathrm{d}t'. \quad (15.11)$$

The visually weighted contrast energy of the $i$th channel is given by

$$\mathcal{E}_{\mathrm{L},i}(I_{\mathrm{L}},x,y,t) = \int a_{\mathrm{L},i}(x'-x,y'-y)|I_{\mathrm{L},i}(x',y',t)|^{\gamma}dx'dy', \quad (15.12)$$

where $a_{\mathrm{L},i}(x,y)$ is a large-space constant spatial filter. The TCE, $\mathcal{E}_{\mathrm{L}}(I_{\mathrm{L}})$ is the weighted sum over all spatial-frequency-and-orientation channels, i.e.

$$\mathcal{E}_{\mathrm{L}}(I_{\mathrm{L}},x,y,t) = \sum_i b_{\mathrm{L},i}\mathcal{E}_{\mathrm{L},i}(I_{\mathrm{L}},x,y,t), \quad (15.13)$$

where $b_{\mathrm{L},i}$ is a gain-control weight that is specific to an output channel (e.g. the horizontal channel centered at 0.68 cpd).

### 15.9.4 How the gain-control model accounts for the data of experiment 1

The model deals with contrast energy $\mathcal{E}$ which, in experiment 1, is taken to be simply the contrast of the sinewave grating stimulus to each eye, $m_{\mathrm{L}}$ and $m_{\mathrm{R}}$. We have $\mathcal{E}_{\mathrm{L}} = b_S m_{\mathrm{L}}^{\gamma}$ and $\mathcal{E}_{\mathrm{R}} = b_S m_{\mathrm{R}}^{\gamma}$, where $b_S$ is the gain-control efficiency of the signal sinewave grating. In experiment 1, even the lowest-contrast stimuli are sufficiently strong that the total contrast energy $\mathcal{E}_{\mathrm{L}}(I_{\mathrm{L}}) \gg 1$. Therefore we can use Eq. (15.10) to fit the data of experiment 1. Given the estimated parameters, using Eq. (15.10) instead of Eq. (15.9) changes the predictions by less than 1%. Equation (15.10) is further simplified to yield:

$$\hat{I} \approx \frac{m_{\mathrm{L}}^{\gamma}}{m_{\mathrm{L}}^{\gamma}+m_{\mathrm{R}}^{\gamma}}I_{\mathrm{L}} + \frac{m_{\mathrm{R}}^{\gamma}}{m_{\mathrm{L}}^{\gamma}+m_{\mathrm{R}}^{\gamma}}I_{\mathrm{R}}. \quad (15.14)$$

The advantage of Eq. (15.14) over Eq. (15.9 ) is that together with Eqs. (15.1) and (15.2) it yields a simple expression for the perceived phase shift $\hat{\theta}$

$$\hat{\theta} \approx 2\tan^{-1}\left(\frac{1-\delta^{\gamma+1}}{1+\delta^{\gamma+1}}\tan\left(\frac{\theta}{2}\right)\right), \quad (15.15)$$

represented by the solid curves in Figures 15.6–15.8. Equations (15.15) and (15.8) yield the effective interocular contrast ratio as a power function of the actual interocular contrast ratio:

$$\hat{\delta} = \delta^{1+\gamma}, \quad (15.16)$$

which is plotted as solid lines in Figure 15.9 along with experimental data. In experiment 1, when $\mathcal{E}_{\mathrm{L}}(I_{\mathrm{L}}) \gg 1$ and $\mathcal{E}_{\mathrm{R}}(I_{\mathrm{R}}) \gg 1$, the gain control effectively attenuates the lower-contrast stimulus by a factor of $\delta^{\gamma}$.

Using Eq. (15.14) (the close approximation for above-threshold stimuli to the full gain-control model) to fit the data, means only one free parameter $\gamma$ needs to be estimated for each observer: $\gamma = 1.18$ for the observer JD whose data are shown in

Figure 15.6; $\gamma = 1.17$ for the observer NS in Figure 15.7; $\gamma = 2.27$ for the observer HT in Figure 15.8. Overall, this 1-estimated-parameter version of the gain-control model accounts for 99.4%, 99.0%, and 98.5%, respectively, of the variance of the data (48 conditions) for observers JD, HT, and NS.

### 15.9.5 How the gain-control model accounts for the data of experiment 2

The data of experiment 2 depend on the temporal filter $h(t)$

$$h(t) = \exp\left(\frac{-t}{\tau}\right), \tag{15.17}$$

in the model as shown in Figure 15.22b. For a pulse of duration $T$ (Eq.( 15.3)), the model output is given by

$$q(t) = \int_0^t u(t')h(t-t')\mathrm{d}t'. \tag{15.18}$$

When inputs $I_{\mathrm{L}}(x,y,t)$ and $I_{\mathrm{R}}(x,y,t)$ are given by Eqs. (15.1) and (15.2), the contrast energies $\mathcal{E}_{\mathrm{L}}(t)$ and $\mathcal{E}_{\mathrm{R}}(t)$ are given by

$$\mathcal{E}_{\mathrm{L}}(t) = b_S\left(m_{\mathrm{L}}\int_0^t u(t')h(t-t')\mathrm{d}t'\right)^{\gamma} = b_S m_{\mathrm{L}}^{\gamma} q^{\gamma}(t), \tag{15.19}$$

$$\mathcal{E}_{\mathrm{R}}(t) = b_S\left(m_{\mathrm{R}}\int_0^t u(t')h(t-t')\mathrm{d}t'\right)^{\gamma} = b_S m_{\mathrm{R}}^{\gamma} q^{\gamma}(t). \tag{15.20}$$

From Eqs. (15.9), (15.19) and (15.20), a cyclopean stimulus $\hat{I}(x,y,t)$ is given by

$$\begin{aligned}\hat{I}(x,y,t) = {} & \frac{k+m_{\mathrm{L}}^{\gamma}q^{\gamma}(t)}{k+m_{\mathrm{L}}^{\gamma}q^{\gamma}(t)+m_{\mathrm{R}}^{\gamma}q^{\gamma}(t)} I_{\mathrm{L}}(x,y,t) + \\ & \frac{k+m_{\mathrm{R}}^{\gamma}q^{\gamma}(t)}{k+m_{\mathrm{L}}^{\gamma}q^{\gamma}(t)+m_{\mathrm{R}}^{\gamma}q^{\gamma}(t)} I_{\mathrm{R}}(x,y,t),\end{aligned} \tag{15.21}$$

where $k = 1/b_S$ is a gain-control threshold energy. Integrating $\hat{I}(x,y,t)$ over stimulus duration $T$ yields $\hat{I}(x,y)$, i.e.

$$\hat{I}(x,y) = \int_0^T \hat{I}(x,y,t)\mathrm{d}t, \tag{15.22}$$

a cyclopean sinewave grating whose phase is used to fit the data.

When the stimulus duration $T$ is very brief, the output of temporal filter $h(t)$ is very small, and the total contrast energy TCE is too small to exert effective gain control in binocular combination; the behavior of the model approximates linear summation. As $T$ increases, the contrast energy also increases, and the behavior of the model deviates from linear summation to become more and more nonlinear.

To fit the data of experiment 2, two new model parameters are needed in addition to the power-law rectification parameter $\gamma$ from experiment 1: a threshold parameter

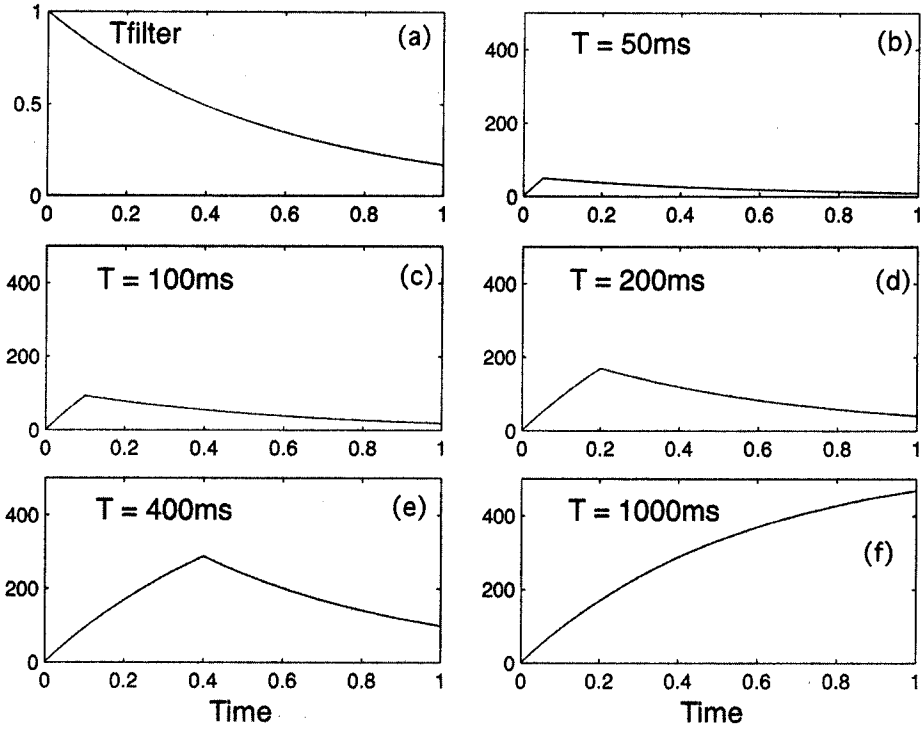


Figure 15.23. The temporal filter (TF) in the gain control circuit and the filter's response to square-wave stimuli of various durations. (a) Impulse response of the temporal filter. A time constant of 563 ms provides an optimal fit to the data of experiment 2. (b)–(f) Filter outputs when the input is a pulse of the indicated duration. In the model, the direct stimulus inputs are not subjected to frequency filtering – an adequate approximation for the current experiments – but the inputs are modified by gain control. In experiment 2, the input is zero when there is no stimulus; therefore gain control is effective only during the actual duration of the stimulus.

$k$, and the time-constant $\tau$ of the temporal filter. The best fitting parameters for data in Figure 15.11 are $\gamma = 2.04$, $k = 2.18 \times 10^{-4}$ s (e.g. 50 ms × 0.436%), and $\tau = 563$ ms. Figure 15.23a illustrates the simple exponential temporal filter, and Figures 15.23b-f illustrate its outputs as stimulus duration $T$ varies from 50 ms to 1 000 ms. The percents of data variance accounted for by the model are 99.4% and 98.2%, respectively, for observers JD and HT.

### 15.9.6 How the gain-control model accounts for the data of experiment 3

In experiment 3, the contrasts of the sinewave grating stimuli to each eye were identical, i.e. $m_R = m_L = m$. Let the RMS contrast of a bandpass noise added to one eye, say

the left eye, be $n$. The total contrast energy is $\mathcal{E}_{\text{L}} = b_S m^\gamma + b_N n^\gamma$ and $\mathcal{E}_{\text{R}} = b_S m^\gamma$. In experiment 3, the contrast energy $\mathcal{E}_{\text{L}} \gg 1$ and $\mathcal{E}_{\text{R}} \gg 1$, so for simplicity, we can use Eq. (15.10). Equation (15.10) becomes

$$\hat{I} = \frac{1 + b(f_{s,N})(N/S)^\gamma}{2 + b(f_{s,N})(N/S)^\gamma} I_{\text{L}} + \frac{1}{2 + b(f_{s,N})(N/S)^\gamma} I_{\text{R}}, \tag{15.23}$$

where $N/S = n/m$ is a noise-to-signal RMS contrast ratio (here, $m$ is defined as RMS contrast), and $b(f_{s,N}) = b_N/b_S$ is a relative contribution to gain control of the bandpass noise with central frequency of $f_{s,N}$. The free parameters for the model are $\gamma_3$ which is the average rectification power-law exponent for the signal and the various noise channels involved in experiment 3, and the $b(f_{s,N})$ that represent the domination efficiencies (relative to the 0.68 cpd horizontal sinewave grating being judged) of the various masking noise stimuli. The six solid curves in Figure 15.14 are the best fits using the gain-control model of Eq. (15.23). For observer JD, the best fitting parameters are $\gamma = 1.89$ and $b(f_{s,N}) = \{0.69, 1.0, 1.68, 3.61, 1.41, 0.42\}$; they yield the spatial frequency modulation transfer function (MTF) illustrated in the top of Figure 15.24. The bottom panel of Figure 15.24 shows the MTF for observer HT. For both observers, the gain-control efficiency of masking noise was at maximum when the noise frequency was at 2.72 cpd (4× the signal spatial frequency). The percents of data variance accounted for by the model are 99.3% and 98.4%, respectively, for observers JD and HT.

### 15.9.7 How the gain-control model accounts for the data of experiments 4–6

In experiments 4–6, when a mask sinewave grating was superimposed on, say, the left eye, the total contrast energy to each eye can be calculated similarly to experiment 3 as $\mathcal{E}_{\text{L}} = b_S m^\gamma + b_M n^\gamma$ and $\mathcal{E}_{\text{R}} = b_S m^\gamma$. Similarly, for the conditions of experiments 4, 5 and 6, the contrast energy $\mathcal{E}_{\text{L}} \gg 1$ and $\mathcal{E}_{\text{R}} \gg 1$. Again, Eq. (15.10) is sufficiently accurate and it simplifies to

$$\hat{I} = \frac{1 + b(f_{s,mask}, f_{t,mask})(M/S)^\gamma}{2 + b(f_{s,mask}, f_{t,mask})(M/S)^\gamma} I_{\text{L}} + \frac{1}{2 + b(f_{s,mask}, f_{t,mask})(M/S)^\gamma} I_{\text{R}}, \tag{15.24}$$

where $M/S = n/m$ is the mask-to-signal contrast ratio and $b(f_{s,mask}, f_{t,mask}) = b_M/b_S$ is the relative contribution to gain control of a masking sinewave grating.

In experiment 4, the spatial frequency of the masking sinewave grating $f_{s,mask}$ is an independent variable, and other parameters of the mask are constant. In Figure 15.16, the solid curves are the best fit of Eq. (15.24). The parameters are $\gamma_4 = 1.004$ and $b(f_{s,mask}) = \{0.81, 1.13, 2.20, 2.27, 1.97, 0.74\}$. The $b(f_{s,mask})$ are plotted against $f_{s,mask}$ to yield the spatial frequency MTF for observer JD, in Figure 15.25 upper right. Figure 15.25 lower right shows spatial frequency MTF for obsever HT. For both observers, the maximum gain-control efficiency was at $f_{s,mask} = 2.72$ cpd, the same as that for the bandpass noise in experiment 3. The percents of data variance accounted for by the model are 98.6% and 97.7%, respectively, for the observers JD and HT.

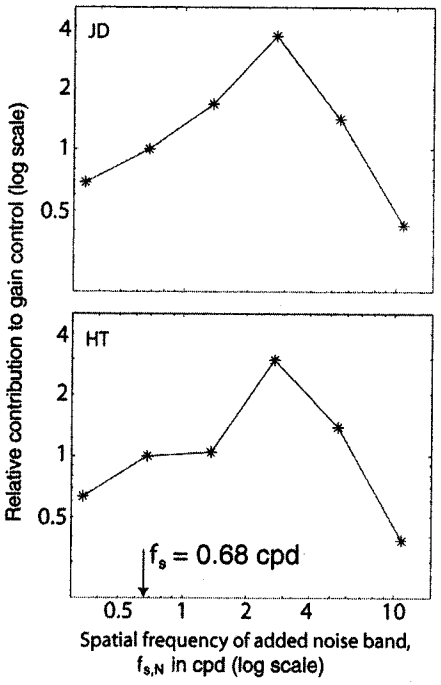


Figure 15.24. How noise of different spatial frequencies increases the weight in binocular combination of the eye to which it is added. Noise in one eye (like all other stimuli) exerts gain control on the opposing eye. The ordinate shows the contribution to gain control, relative to the stimulus grating being judged (0.68 cpd), of the added noise as derived from the gain-control model. The abscissa indicates the central frequency of the added noise. Based on data of experiment 3 for two observers. For both observers, maximum gain-control efficiency occurred at 2.72 cpd (4× the signal frequency).

In the left column of Figure 15.25 the perceived phase shift $\hat{\theta}$ is plotted against $f_{s,mask}$ at different contrast levels. For both observers, at low contrast levels, the curves have peaks at $f_{s,mask} = 2.72$ cpd. However, at high contrast levels, the curves are flat; the contrast efficiencies are similar for all spatial frequencies.

In experiment 5 the temporal frequency of the masking sinewave grating $f_{t,mask}$ is an independent variable, and the other mask parameters are constant. In Figure 15.18, the solid curves are the best fits using Eq. (15.24). The best fitting parameters are $\gamma_5 = 1.43$ and $b(f_{t,mask}) = \{1.06, 1.54, 1.72, 1.74, 0.49\}$, which are plotted against $f_{t,mask}$ to yield the temporal frequency MTF for observer JD in Figure 15.26 upper right. Figure 15.26 lower right shows temporal frequency MTF for obsever HT. For both observers, the corner frequency was about 15 Hz. In the left column of Figure 15.26, the perceived phase shift $\hat{\theta}$ is plotted against $f_{t,mask}$ at different contrast levels; at low contrast levels, the corner frequency is at 15 Hz, but at high contrast levels, the MTF becomes quite flat. The percents of data variance accounted for by the model are 99.2% and 99.3%, respectively, for observers JD and HT.

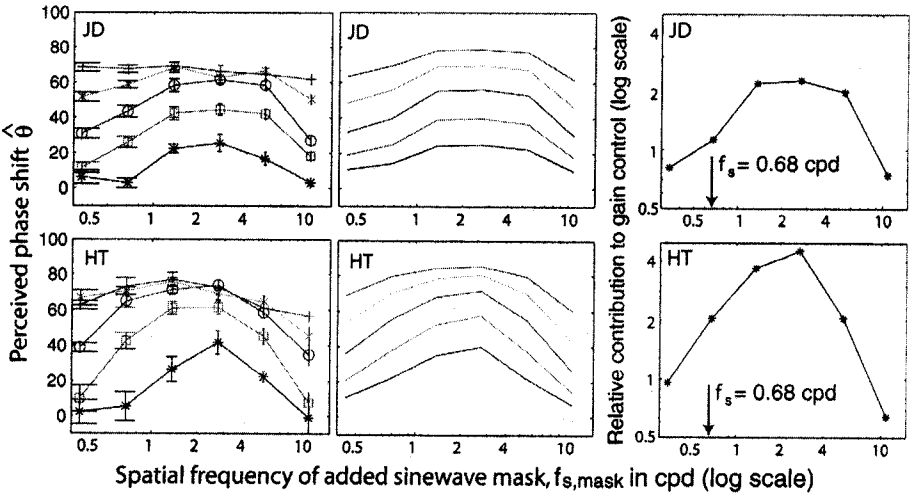


Figure 15.25. The transformation of a single gain-control efficiency function for spatial frequency masking into multiple modulation transfer functions that depend on stimulus contrast. (Left column) Spatial frequency modulation transfer functions. Perceived phase shift $\hat{\theta}$ as a function of the spatial frequency of a masking sine wave grating added in one eye, shown for mask contrast amplitudes of 2.5% (∗), 5% (□), 10% (○), 20% (×), and 40% (+). (Right column) Gain-control efficiency of a masking grating in one eye as a function of its spatial frequency. These efficiencies (weighting parameters in the gain-control model) are used to fit the model to the data of experiment 4, i.e. to generate the predicted perceived phase shifts $\hat{\theta}$ in the center column, which are the gain-control model's best fits to the data panels on the left. Observers JD, HT.

For experiment 6, the orientation $\beta$ of the masking sinewave grating, is an independent variable, and other parameters of the mask are fixed. In Figure 15.27, the solid curves in the center panels are the best fits derived from Eq. (15.24). The best fitting parameters are $\gamma_6 = 1.42$ and $b(\beta) = \{1.92, 1.21, 1.13, 1.52, 2.11, 1.54, 0.81, 1.06, 2.07\}$; these are plotted against orientation $\beta$ in Figure 15.27 upper right to yield the orientation tuning function for observer JD. Figure 15.27 (lower right) shows the orientation tuning function for observer HT. For both observers, the vertical and horizontal gratings contributed more to the total contrast energy than the gratings in $\pm 45°$ orientations. In the left column of Figure 15.27, the perceived phase shift $\hat{\theta}$ is plotted against $\beta$ at different contrast levels. The percents of data variance accounted for by the model are 98.6% and 96.9%, respectively, for observers JD and HT.

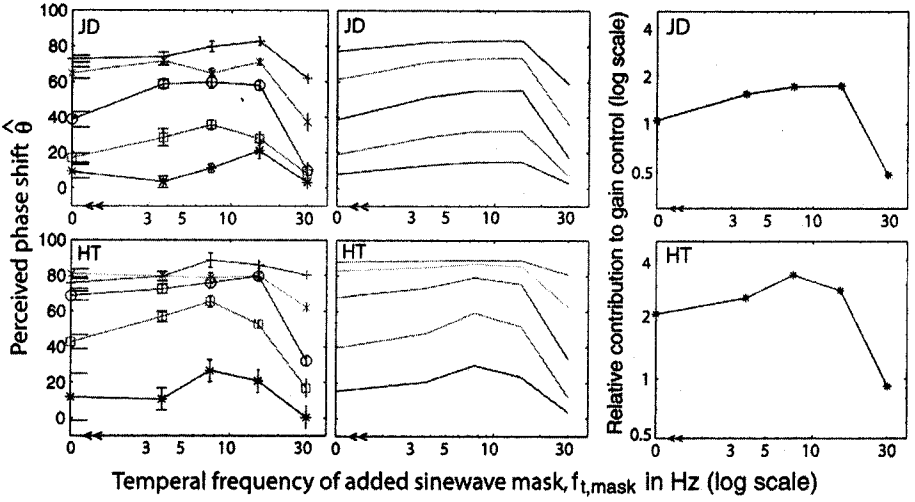


Figure 15.26. The transformation of a single gain-control efficiency function for temporal frequency masking into multiple modulation transfer functions that depend on stimulus contrast. (Left column) Temporal frequency modulation transfer functions. Perceived phase shift $\hat{\theta}$ as a function of the temporal frequency of a masking sine wave grating added to one eye, shown for mask contrast levels of 2.5% (∗), 5% (□), 10% (○), 20% (×), and 40% (+). (Right column) Gain-control efficiency of a masking grating in one eye as a function of its temporal frequency. These efficiencies (weighting parameters in the gain-control model) are used to fit the model to the data of experiment 5, i.e. to generate the predicted perceived phase shifts $\hat{\theta}$ in the center column, which are the gain-control model's best fits to data panels on the left. Observers JD, HT.

# 15.10 Discussion

## 15.10.1 Binocular iso-contrast contours

The present experiments have not dealt with amplitude, only with phase, i.e. the perceived location of the dark stripe of a cyclopean grating. Here we investigate the gain-control model's predictions for the perceived contrast of cyclopean gratings, specifically, iso-contrast contours.

Consider sinewave gratings, identical except for contrast, that are presented to the left and right eyes, i.e., $I_{\text{L}} = m_{\text{L}} \sin x$ and $I_{\text{R}} = m_{\text{R}} \sin x$. According to the model, $\mathcal{E}_{\text{L}}(I_{\text{L}}) = b m_{\text{L}}^{\gamma}$ and $\mathcal{E}_{\text{R}}(I_{\text{R}}) = b m_{\text{R}}^{\gamma}$. To simplify the expressions, replace $k$ with $1/b$. This yields an expression for the perceived cyclopean contrast $\hat{m}$

$$\hat{m} = \frac{k + m_{\text{L}}^{\gamma}}{k + m_{\text{L}}^{\gamma} + m_{\text{R}}^{\gamma}} m_{\text{L}} + \frac{k + m_{\text{R}}^{\gamma}}{k + m_{\text{L}}^{\gamma} + m_{\text{R}}^{\gamma}} m_{\text{R}}. \tag{15.25}$$

At very low contrast-energy levels, $m_{\text{L}}^{\gamma} \ll k$ and $m_{\text{R}}^{\gamma} \ll k$, the equal contrast contours

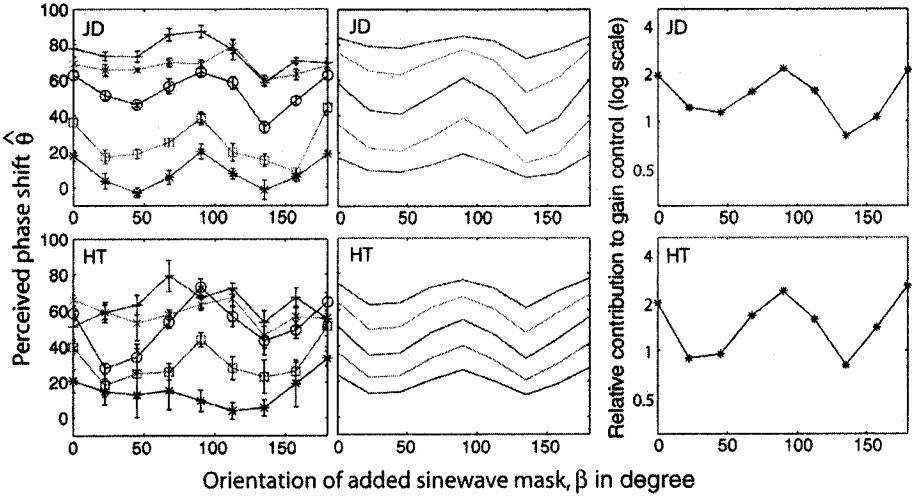


Figure 15.27. The transformation of a single gain-control efficiency function for orientation masking into multiple modulation transfer functions that depend on stimulus contrast. (Left column) Orientation modulation transfer functions: Perceived phase shift $\hat{\theta}$ as a function of the angle relative to the horizontal stimulus being judged of a masking sine wave grating added to one eye, shown for contrasts of 2.5% (∗), 5% (□), 10% (○), 20% (×), and 40% (+). Zero on the abscissa indicates parallel stimulus and masking gratings. (Right column) Gain-control efficiency of a masking grating in one eye as a function of its orientation relative to the stimulus being judged. These orientation efficiencies (weighting parameters in the gain-control model) are used to fit the model to the data of experiment 6, i.e. to generate the predicted perceived phase shifts $\hat{\theta}$ in the center column, which are the gain-control model's best fits to data panels on the left. Observers JD, HT.

on a graph of $m_R$ versus $m_L$ are almost linear, i.e.

$$\hat{m} \approx m_L + m_R. \tag{15.26}$$

At high contrast-energy levels, $m_L^\gamma \gg k$ and $m_R^\gamma \gg k$, we have,

$$\hat{m} \approx \frac{m_L^\gamma}{m_L^\gamma + m_R^\gamma} m_L + \frac{m_R^\gamma}{m_L^\gamma + m_R^\gamma} m_R, \tag{15.27}$$

which is contrast-weighted summation.

Legge and Rubin (1981) studied binocular combination in a supra-threshold contrast matching task that involved left- and right-eye sinewave gratings with different contrasts combined into a cyclopean grating.

Figure 15.28a shows examples of binocular iso-contrast contours extracted from Legge and Rubin (1981). To smooth their data, all points shown in Figure 15.28a, except the points at the ends of contours, are averaged with their two nearest neighbors. The two resulting contours represent Legge and Rubin's highest and lowest iso-perceived-contrast contours. The dashed line is a prediction of linear summation.

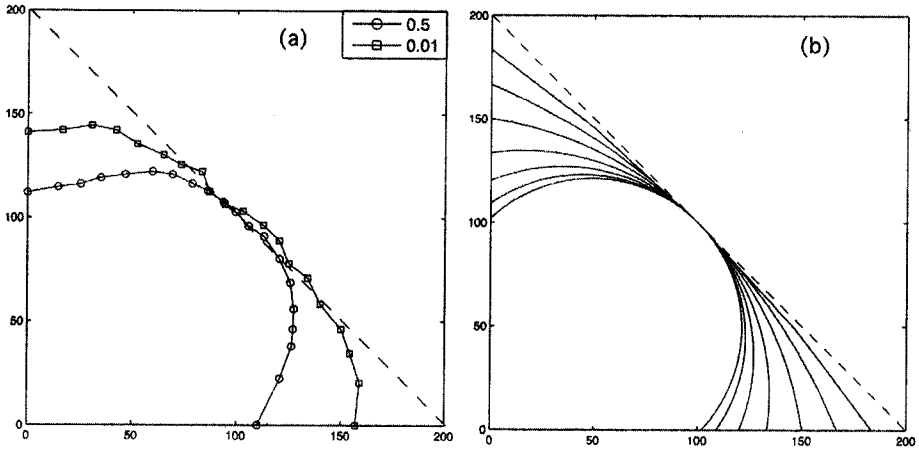


Figure 15.28. Binocular perceived iso-contrast contours. Combinations of left- and right-eye grating contrasts that produce equal cyclopean perceived contrasts. (a) Replot of two binocular iso-contrast contours from Legge and Rubin (1981, Figure 4B, p. 55). Except the data points at the ends of the plot, each plotted point is an average of the original point at that location with its two neighbors. (b) Binocular iso-contrast contours generated by the gain-control model. Sinewave gratings presented to two eyes are identical except for their contrasts. The abscissa is the contrast of the left-eye grating; the ordinate is the contrast of the right-eye grating. The curves are binocular iso-contrast contours. The model parameters are assumed to be $k = 0.02$ s and $\gamma = 1$. The dashed lines are the predictions from linear summation of the contrasts in the two eyes. The solid lines are normalized predictions from the gain-control model at contrast levels of 0.002, 0.005, 0.01, 0.02, 0.04, 0.1, and 0.5 corresponding from top to bottom. Both the model and the data at high (but not at low) contrast exhibit Fechner's paradox; i.e. replacing a zero-contrast stimulus in one eye with a low-contrast stimulus (thereby increasing the total contrast energy presented to the observer) reduces apparent cyclopean contrast and requires an increase in the contrast of the high-contrast grating to maintain perceived iso-contrast.

Figure 15.28b shows the full gamut of iso-perceived-contrast contours derived from a simulation of the gain-control model for various contrast levels from very low contrast (0.002) to very high contrast (0.50) with model parameters $k = 0.02$ and $\gamma = 1$. Generally, the features of the data and of the model correspond very well. At a low contrast level (0.01), the data contour approaches the limiting straight line expected from linear summation at extremely low contrast energies. At a high stimulus contrast level (0.50), the data contour is highly nonlinear and it looks quite similar to the 0.50 contour of the model.

Both the data and the model demonstrate Fechner's paradox in the high-contrast iso-contrast contours but not in low-contrast contours. Fechner observed that when the contrast of the grating in one eye is zero, increasing the contrast in that grating initially decreases the (perceived) cyclopean contrast even though overall contrast energy has

increased. In the model, Fechner's paradox occurs because the gain control from the low-contrast eye has a greater divisive effect in reducing the output of the high-contrast eye than an additive effect in contributing to the summed output, especially as its output is being attenuated by intense gain control from the competing eye which is receiving a high-contrast grating.

### 15.10.2 Binocular power summation

Legge (1984b) proposed a binocular quadratic summation to explain his data derived from binocular combination experiments. Similarly, Anderson and Movshon (1989) reported that, in a binocular detection task for vertical sinewave gratings, the iso-effectiveness contour for binocular summation could be well described by a power-summation equation of the form

$$\hat{m}^{\sigma} = m_{\mathrm{R}}^{\sigma} + m_{\mathrm{L}}^{\sigma}, \tag{15.28}$$

with an exponent $\sigma$ near 2. Binocular power summation implies that the contrast signal in each eye is subjected to a power-law transformation prior to binocular summation. For example, one implication for experiment 1 would be that the effective interocular contrast ratio would be $\hat{\delta} = \delta^{\sigma}$. If we take $\sigma = 1 + \gamma$, it turns out that both the power summation model and the gain-control model give the same effective interocular contrast ratio. This apparently happy coincidence of two theories is superficial. A power-law transform applies only to weak stimuli. For high-contrast stimuli addition of the two eyes' power-law-transformed stimuli would grossly violate the one-eye-equals-both-eyes constraint for equal stimuli to both eyes.

The data of experiment 2 (exposure duration) offer very clear limits on the exponent of a power law that could operate on monocular signals before they were added in binocular combination. We consider here the graphs of $\hat{\theta}$ versus $\delta$ (e.g. Figure 15.11) and a log-log graph of $\hat{\delta}$ versus $\delta$ (e.g. Figure 15.13). Data from threshold-level stimuli were not obtained here but experiment 2 provides data concerning the binocular summation of fairly low contrast-energy stimuli in the condition: exposure duration 50 ms, grating contrast 0.10. In Figure 15.29, these data from experiment 2 are displayed on the two graphical forms described above. The solid line is the best fit from the gain-control model. The dashed lines are predictions from a power-summation model (Eq. (15.28)) with power-law exponent $\sigma = \{1, 1.2, 1.4, 1.7, 2, 2.5, 3\}$ corresponding to the dashed lines from bottom to top in Figure 15.29a and from top to bottom in Figure 15.29b. With the possible exception of a point for $\delta$= 0.2 (where log variability is greatest), the data are consistent with a power-law exponent of 1.0, and clearly rule out exponents greater than 1.20. The conclusion is that monocular inputs, at least from grating stimuli, combine linearly, or nearly so, prior to binocular combination. Apparent similarity (when it occurs) to a power-law transformation prior to binocular combination derives from quite different processes.

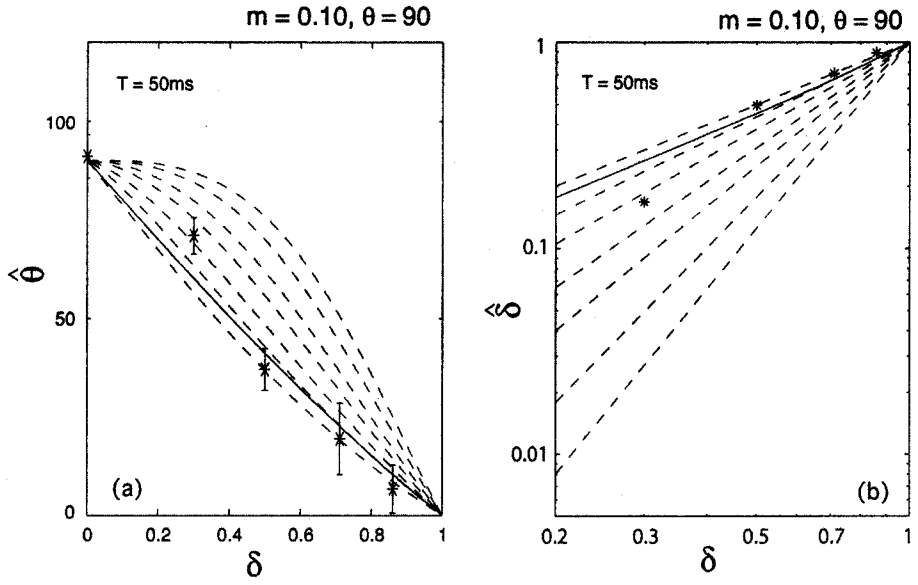


Figure 15.29. Is the monocular signal transformed nonlinearly by a power law prior to binocular combination? Comparison of the gain-control model with a power-law transformation. Power-law transformations are most effective at near-threshold contrasts, so we consider the subset of data from experiment 2, Figure 15.11, in which the contrast of the higher-contrast grating is 0.1, the contrast of the lower-contrast grating is $0.1\delta$ and the exposure duration is 50 ms (the lowest energy stimuli tested). The solid curve is the prediction of the gain-control model (linear transduction, no input power-law transformation). The dashed lines are predictions from a power-law transduction model with power-law exponents $\sigma$ = 1, 1.2, 1.4, 1.7, 2, 2.5, 3 corresponding to the dashed lines from bottom to top. (b) A log-log plot of the apparent interocular contrast ratio $\hat{\delta}$ as a function of the actual interocular contrast ratio $\delta$. The solid curve is a prediction of the gain-control model; the dashed lines are predictions based on a power-law transformation prior to binocular combination with power-law exponents $\sigma$ = 1, 1.2, 1.4, 1.7, 2, 2.5, 3 corresponding to the dashed lines from top to bottom. Conclusion: Prior to binocular combination, the input contrast is represented linearly or very nearly linearly.

## 15.11 Summary and conclusions

Six experiments were performed. In experiment 1, static sinewave gratings of different modulation contrasts and in different phases were presented to the left and right eyes. Stimuli were viewed for 1 s. The data consist of 48 combinations of contrasts of the left- and right-eye stimuli and of their relative phases. From the judged phase of the cyclopean grating relative to a reference marker, we inferred the ratio of the contributions of the two eyes to the cyclopean image. In all cases, the stimulus with greater contrast had more weight in binocular combination than predicted by simple linear summation.

A one-parameter gain-control model accounted for 98% of the variance of the data. The gain-control model predicts that when the contrast energy is much smaller than a particular constant in the gain-control equation, binocular combination will be perfectly described by linear summation. The deviations from perfect summation (nonlinearity) become increasingly important as the contrast energy of the stimulus increases. The model also correctly predicts that for idential stimuli to both eyes at moderate and high contrasts, the perceived cyclopean image will be the same whether viewed with one or both eyes.

Experiment 2 investagated the effect of varying grating contrast and exposure duration as multiplicative contributers to contrast energy. The stimuli and procedure were similar to experiment 1 except that the duration was varied in the range from 50 ms to 1000 ms to create low-energy stimuli (50 ms, contrast 0.1) ranging to very strong stimuli (1000 ms, contrast 0.2). The results show that for low-contrast-energy stimuli binocular combination is well described by algebraic summation of the two physical images – no gain control is observed. As stimulus duration and/or contrast is increased, algebraic summation of left- and right-eye images increasingly fails to account for perception. This increasing deviation of observed binocular combination from linear summation is well modeled by a gain-control pathway that has an exponential decay filter with a time constant of 563 ms.

Experiment 3 investigated the question: When the spatial frequency for which binocular combination is being determined is $f_0$, how much do other spatial frequencies $f_1$ contribute to gain control? Each eye was presented with a sinewave grating, the interocular phase difference was 90°, and bandpass spatial noise was added to the grating in one eye. The eye with the added noise dominated binocular combination. Noise in a 4× higher frequency band than the signal being judged was the most effective stimulus for producing dominance. Adding noise is inconsistent with a Bayesian model that would give less weight to noisy signals, but it is totally consistent with a gain-control model in which Total visually weighted Contrast Energy (TCE) determines the interocular gain control.

Experiments 4–6 were designed to measure the contribution of various frequency components to TCE and thereby to ocular dominance. The paradigms were the same as in experiment 3 in that 90°. out-of-phase grating stimuli were presented to both eyes and a masking grating was added to only one eye's stimulus. The contrasts of the masking sinewave gratings were varied. Experiment 4 also varied the spatial frequency of a sinewave masking grating that was perpendicular to the grating whose phase was being judged and it produced similar results to experiment 3 in which bandpass noise was added. Experiment 5 varied the temporal frequency to reveal a low-pass characteristic with a corner frequency of about 15 Hz. Experiment 6 varied orientation. Spatial, temporal, and orientation modulation transfer functions were derived to describe the TCE gain-control parameters and thereby to characterize the increase in dominance provided by the various masking stimuli. The gain-control model accurately described the change in dominance as the ratio of the two eyes' contrasts varied and as the overall contrast energy level varied, accounting for at least 97% of the data variance for all observers in all experiments. In experiment 6, added orientation gratings were most effective at inceasing ocular dominance when their orientation was vertical or horizontal versus diagonal, implicating at least a partial cortical origin for interocular gain control.

# References and further reading

Anderson, P. A. and Movshon, J. A. (1989). Binocular combination of contrast signals. *Vis. Res.*, **29**, 1115–1132.

Bearse Jr., M. A. and Freeman, R. D. (1994). Binocular summation in orientation discrimination depends on stimulus contrast and duration *Vis. Res.*, **34**, 19–29.

Blake, R. (2003). In L. M. Chalupa and J. Warner, eds., *The Visual Neurosciences*. Cambridge, MA: MIT Press.

Bolanowski Jr., S. J. (1987). Contourless stimuli produce binocular brightness summation. *Vis. Res.*, **27**, 1943–1951.

Brainard, D. H. (1997). The Psychophysics Toolbox, *Spat. Vis.*, **10**, 433–436.

De Weert, C. M. M. and Levelt, W. J. M. (1974) Binocular brightness combinations: Additive and nonadditive aspects. *Percept. Psychophys.*, **15**, 551–562.

Ding, J. and Sperling, G. (2006). A gain-control theory of binocular combination. *Proc. Natl. Acad. Sci. USA*, **103**, 1141–1146.

Finney, D. J. (1971), *Probit Analysis*, third edition. Cambridge: Cambridge University Press.

Legge, G. E. (1979). Spatial frequency masking in human vision: binocular interactions. *J. Opt. Soc. Am. A*, **69**, 838–847.

Legge, G. E. (1984a). Binocular contrast summation–I. Detection and discrimination *Vis. Res.*, **24**, 373–383.

Legge, G. E. (1984b). Binocular contrast summation–II. Quadratic summation *Vis. Res.*, **24**, 373–383.

Legge, G. E. and Rubin, G. S. (1981). Binocular interactions in suprathreshold contrast perception. *Percept. Psychophys.*, **30**, 49–61.

Levelt, W. J. M. (1965a). *On Binocular Rivalry*. Institute for Perception RVO-TNO, Soesterberg, The Netherlands.

Levelt, W. J. M. (1965b). Binocular brightness averaging and contour information. *British J. Psych.*, **56**, 1–13.

Lu, Z. L. and Sperling, G. (1999). Second-order reversed phi. *Percept. Psychophys.*, **61**, 1075–1088.

Mansfield, J. S. and Legge, G. E. (1996). The binocular computation of visual direction. *Vis. Res.*, **36**, 27–41.

Pelli, D. G. (1997). The VideoToolbox software for visual psychophysics: Transforming numbers into movies. *Spat. Vis.*, **10**, 437–442.

Pelli, D. G. and Zhang, L. (1991). Accurate control of contrast on microcomputer displays. *Vis. Res.*, **31**, 1337–1350.

Rainville, S. J. M. and Kingdom, F. A. A. (2002) Scale invariance is driven by stimulus density. *Vis. Res.*, **42**, 351–367.